USGS
science for a changing world

Geologic Field-Trip Guide to Mount Shasta Volcano, Northern California

Scientific Investigations Report 2017–5022–K3

U.S. Department of the Interior
U.S. Geological Survey

Cover: Aerial view from the north across the Shasta Valley sector-collapse debris-avalanche deposit, with Mount Shasta and Black Butte rising in the background. Photograph by J. Scurlock.

Geologic Field-Trip Guide to Mount Shasta Volcano, Northern California

By Robert L. Christiansen, Andrew T. Calvert, and Timothy L. Grove

Scientific Investigations Report 2017–5022–K3

U.S. Department of the Interior
U.S. Geological Survey

U.S. Department of the Interior
RYAN K. ZINKE, Secretary

U.S. Geological Survey
William H. Werkheiser, Acting Director

U.S. Geological Survey, Reston, Virginia: 2017

Suggested citation:
Christiansen, R.L., Calvert, A.T., and Grove T.L., 2017, Geologic field-trip guide to Mount Shasta volcano, northern California: U.S. Geological Survey Scientific Investigations Report 2017-5022-K3, 33 p., https://doi.org/10.3133/sir20175022K3.

ISSN 2328-0328 (online)

Preface

The North American Cordillera is home to a greater diversity of volcanic provinces than any comparably sized region in the world. The interplay between changing plate-margin interactions, tectonic complexity, intra-crustal magma differentiation, and mantle melting have resulted in a wealth of volcanic landscapes. Field trips in this series visit many of these landscapes, including (1) active subduction-related arc volcanoes in the Cascade Range; (2) flood basalts of the Columbia Plateau; (3) bimodal volcanism of the Snake River Plain-Yellowstone volcanic system; (4) some of the world's largest known ignimbrites from southern Utah, central Colorado, and northern Nevada; (5) extension-related volcanism in the Rio Grande Rift and Basin and Range Province; and (6) the spectacular eastern Sierra Nevada featuring Long Valley Caldera and the iconic Bishop Tuff. Some of the field trips focus on volcanic eruptive and emplacement processes, calling attention to the fact that the western United States provides opportunities to examine a wide range of volcanological phenomena at many scales.

The 2017 Scientific Assembly of the International Association of Volcanology and Chemistry of the Earth's Interior (IAVCEI) in Portland, Oregon, marks the first time that the U.S. volcanological community has hosted this quadrennial meeting since 1989, when it was held in Santa Fe, New Mexico. The 1989 field-trip guides are still widely used by students and professionals alike. This new set of field guides is similarly a legacy collection that summarizes decades of advances in our understanding of magmatic and tectonic processes of volcanic western North America.

The field of volcanology has flourished since the 1989 IAVCEI meeting, and it has profited from detailed field investigations coupled with emerging new analytical methods. Mapping has been enhanced by plentiful major- and trace-element whole-rock and mineral data, technical advances in radiometric dating and collection of isotopic data, GPS (Global Positioning System) advances, and the availability of lidar (light detection and ranging) imagery. Spectacularly effective microbeam instruments, geodetic and geophysical data collection and processing, paleomagnetic determinations, and modeling capabilities have combined with mapping to provide new information and insights over the past 30 years. The collective works of the international community have made it possible to prepare wholly new guides to areas across the western United States. These comprehensive field guides are available, in large part, because of enormous contributions from many experienced geologists who have devoted entire careers to their field areas. Early career scientists are carrying forward and refining their foundational work with impressive results.

Our hope is that future generations of scientists as well as the general public will use these field guides as introductions to these fascinating areas and will be enticed toward further exploration and field-based research.

Michael Dungan, University of Oregon
Judy Fierstein, U.S. Geological Survey
Cynthia Gardner, U.S. Geological Survey
Dennis Geist, National Science Foundation
Anita Grunder, Oregon State University
John Wolff, Washington State University

Field-trip committee, IAVCEI 2017

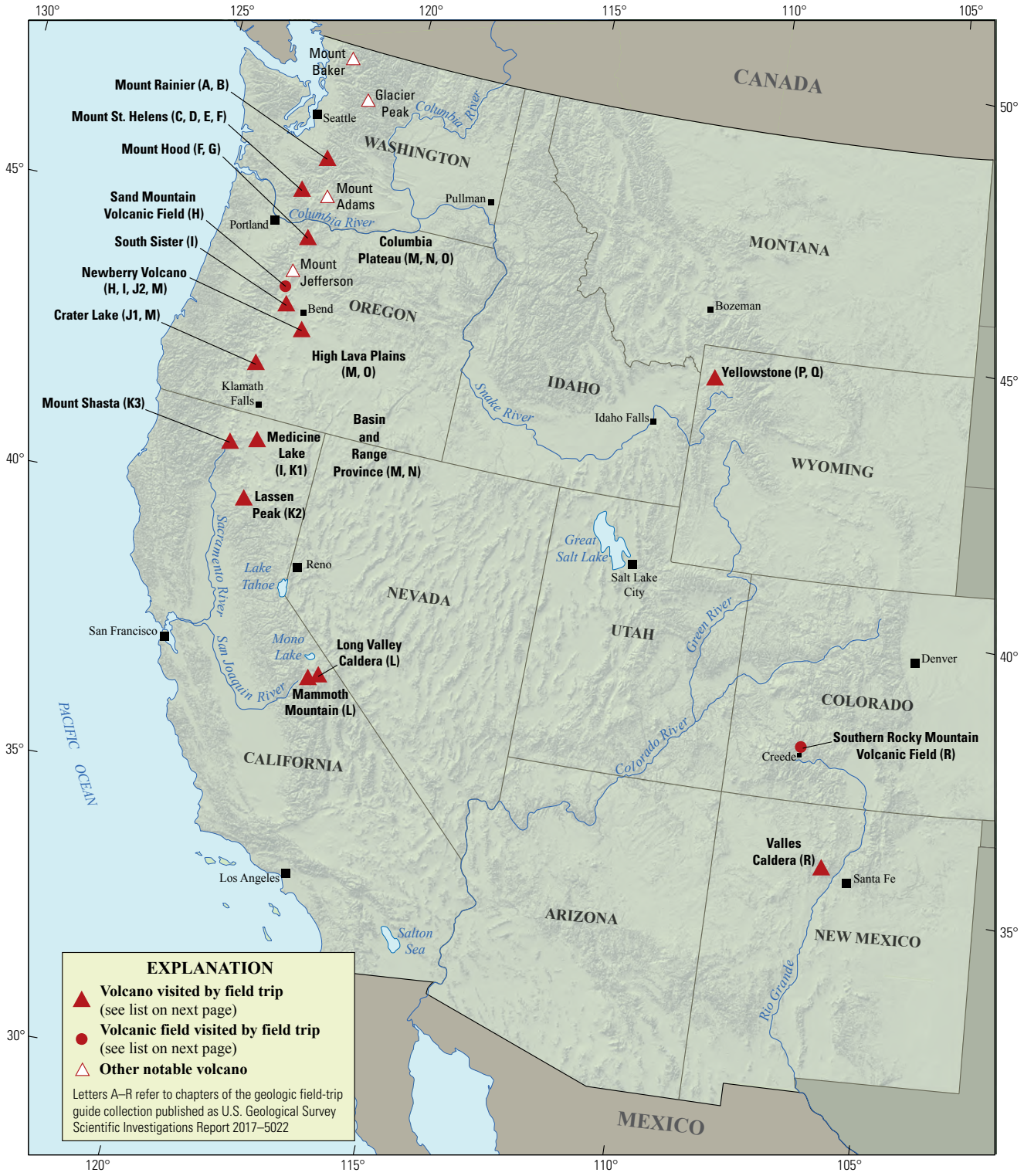

Map of the western United States showing volcanoes and volcanic fields visited by geologic field trips scheduled in conjunction with the 2017 meeting of the International Association of Volcanology and Chemistry of the Earth's Interior (IAVCEI) in Portland, Oregon, and available as chapters in U.S. Geological Survey Scientific Investigations Report 2017–5022. Shaded-relief base from U.S. Geological Survey National Elevation Dataset 30-meter digital elevation model data.

Contributing Authors

Boise State University
Brittany D. Brand
Nicholas Pollock

Colgate University
Karen Harpp
Alison Koleszar

Durham University
Richard J. Brown

Eastern Oregon University
Mark L. Ferns

ETH Zurich
Olivier Bachmann

Georgia Institute of Technology
Josef Dufek

GNS Science, New Zealand
Natalia I. Deligne

Hamilton College
Richard M. Conrey

Massachusetts Institute of Technology
Timothy Grove

National Science Foundation
Dennis Geist (also with Colgate University and University of Idaho)

New Mexico Bureau of Geology and Mineral Resources
Paul W. Bauer
William C. McIntosh
Matthew J. Zimmerer

New Mexico State University
Emily R. Johnson

Northeastern University
Martin E. Ross

Oregon Department of Geology and Mineral Industries
William J. Burns
Lina Ma
Ian P. Madin
Jason D. McClaughry

Oregon State University
Adam J.R. Kent

Portland State University
Jonathan H. Fink (also with University of British Columbia)
Martin J. Streck
Ashley R. Streig

San Diego State University
Victor E. Camp

Smithsonian Institution
Lee Siebert

Universidad Nacional Autónoma de San Luis Potosi
Damiano Sarocchi

University of California, Davis
Kari M. Cooper

University of Liverpool
Peter B. Kokelaar

University of Northern Colorado
Steven W. Anderson

University of Oregon
Ilya N. Binderman
Michael A. Dungan
Daniele Mckay (also with Oregon State University and Oregon State University, Cascades)

University of Portland
Kristin Sweeney

University of Tasmania
Martin Jutzeler
Jocelyn McPhie

University of Utah
Jamie Farrell

U.S. Army Corps of Engineers
Keith I. Kelson

U.S. Forest Service
Gordon E. Grant (also with Oregon State University)

U.S. Geological Survey
Charles R. Bacon
Andrew T. Calvert
Christine F. Chan
Robert L. Christiansen
Michael A. Clynne
Michael A. Cosca
Julie M. Donnelly-Nolan
Benjamin J. Drenth
William C. Evans
Judy Fierstein
Cynthia A. Gardner
V.J.S. Grauch
Christopher J. Harpel
Wes Hildreth
Richard P. Hoblitt
Robert A. Jensen
Peter W. Lipman
Jacob B. Lowenstern
Jon J. Major
Seth C. Moran
Lisa A. Morgan
Leah E. Morgan
L.J. Patrick Muffler
Jim O'Connor
John S. Pallister
Thomas C. Pierson
Joel E. Robinson
Juliet Ryan-Davis
Kevin M. Scott
William E. Scott
Wayne (Pat) Shanks
David R. Sherrod
Thomas W. Sisson
Mark Evan Stelten
Weston Thelen
Ren A. Thompson
Kenzie J. Turner
James W. Vallance
Alexa R. Van Eaton
Jorge A. Vazquez
Richard B. Waitt
Heather M. Wright

U.S. Nuclear Regulatory Commission
Stephen Self (also with University of California, Berkeley)

Washington State University
Joseph R. Boro
Owen K. Neill
Stephen P. Reidel
John A. Wolff

Acknowledgments
Juliet Ryan-Davis and Kate Sullivan created the overview map, and Vivian Nguyen created the cover design for this collection of field-trip guide books. The field trip committee is grateful for their contributions.

Contents

Figures

Conversion Factors

[International System of Units to U.S. customary units]

Multiply	By	To obtain
	Length	
centimeter (cm)	0.3937	inch (in.)
millimeter (mm)	0.03937	inch (in.)
meter (m)	3.281	foot (ft)
kilometer (km)	0.6214	mile (mi)
meter (m)	1.094	yard (yd)
	Area	
square centimeter (cm^2)	0.001076	square foot (ft^2)
square meter (m^2)	10.76	square foot (ft^2)
square centimeter (cm^2)	0.1550	square inch (ft^2)
square kilometer (km^2)	0.3861	square mile (mi^2)
	Volume	
cubic meter (m^3)	35.31	cubic foot (ft^3)
cubic kilometer (km^3)	0.2399	cubic mile (mi^3)

Temperature in degrees Celsius (°C) may be converted to degrees Fahrenheit (°F) as °F = (1.8 × °C) + 32.

Abbreviations

amph	amphibole
An	anorthite
$^{40}Ar/^{39}Ar$	argon-40/argon-39 age method
BA	basaltic andesite
^{14}C	carbon-14
DEM	digital elevation model
HAOT	high-alumina olivine tholeiite
HMA	high-magnesian (Mg) andesite
ka	kilo-annum or 1,000 (10^3) years
LGM	last glacial maximum
LKOT	low-potassium olivine tholeiite
LREE	light rare-earth element
Ma	mega annum or 1,000,000 (10^6) years
Mg#	100* Mg/Mg + Fe*
MIS	marine oxygen-isotope stage
MORB	mid-ocean-ridge basalt
MPa	1 mega pascal or 1 million pascal
NNO	nickel-nickel oxide
oliv	olivine
PMA	primitive magnesian andesite
pyz	pyroxene
QFM	quartz-fayalite-magnetite
USGS	U.S. Geological Survey

Geologic Field-Trip Guide to Mount Shasta Volcano, Northern California

By Robert L. Christiansen[1], Andrew T. Calvert[1], and Timothy L. Grove[2]

Introduction

The southern part of the Cascades Arc formed in two distinct, extended periods of activity: "High Cascades" volcanoes erupted during about the past 6 million years and were built on a wider platform of Tertiary volcanoes and shallow plutons as old as about 30 Ma, generally called the "Western Cascades." For the most part, the Shasta segment (for example, Hildreth, 2007; segment 4 of Guffanti and Weaver, 1988) of the arc forms a distinct, fairly narrow axis of short-lived small- to moderate-sized High Cascades volcanoes that erupted lavas, mainly of basaltic-andesite or low-silica-andesite compositions. Western Cascades rocks crop out only sparsely in the Shasta segment; almost all of the following descriptions are of High Cascades features except for a few unusual localities where older, Western Cascades rocks are exposed to view along the route of the field trip.

The High Cascades arc axis in this segment of the arc is mainly a relatively narrow band of either monogenetic or short-lived shield volcanoes. The belt generally averages about 15 km wide and traverses the length of the Shasta segment, roughly 100 km between about the Klamath River drainage on the north, near the Oregon-California border, and the McCloud River drainage on the south (fig. 1). Superposed across this axis are two major long-lived stratovolcanoes and the large rear-arc Medicine Lake volcano. One of the stratovolcanoes, the Rainbow Mountain volcano of about 1.5–0.8 Ma, straddles the arc near the midpoint of the Shasta segment. The other, Mount Shasta itself, which ranges from about 700 ka to 0 ka, lies distinctly west of the High Cascades axis. It is notable that Mount Shasta and Medicine Lake volcanoes, although volcanologically and petrologically quite different, span about the same range of ages and bracket the High Cascades axis on the west and east, respectively.

The field trip begins near the southern end of the Shasta segment, where the Lassen Volcanic Center field trip leaves off, in a field of high-alumina olivine tholeiite lavas (HAOTs, referred to elsewhere in this guide as low-potassium olivine tholeiites, LKOTs). It proceeds around the southern, western, and northern flanks of Mount Shasta and onto a part of the arc axis. The stops feature elements of the Mount Shasta area in an approximately chronological order, from oldest to youngest.

Tectonic Setting

The fore-arc region west of Mount Shasta comprises elements of the Klamath Mountains, a stack of thrust-bounded tectonic terranes that consist mainly of ophiolitic rocks and Paleozoic and Mesozoic metasedimentary rocks. Both geologic mapping and a seismic-refraction survey (Zucca and others, 1986; Fuis and others, 1987) indicate that Klamath lithologies underlie the arc in the Shasta segment; Klamath lithologies also occur as sparse xenoliths in some Mount Shasta lavas. A prominent salient of eastern Klamath Mountains rocks, ranging in age from Ordovician to Jurassic, extends eastward along the south side of the Shasta segment, marking the southern extent of High Cascades volcanic vents of the Shasta segment and a volcanic gap of about 50 km that extends south to the northern end of the Lassen segment of the arc.

Because of its location with respect to the arc axis, Mount Shasta is, in effect, a fore-arc volcano. Seismic data (McCrory and others, 2012) indicate that the east-dipping, subducting Gorda Plate lies at a depth of about 70 km beneath Mount Shasta. A more or less equant low-gravity anomaly encompasses much of the Shasta segment, and Mount Shasta itself is centered in a zone within that more regional low, having the lowest gravity values in the region (Pakiser, 1964; LaFehr, 1965). In a somewhat complementary fashion, the Medicine Lake volcano east of the Cascades axis defines a local gravity high within the area of the more regional low.

East of the arc, normal faults related to basin-range tectonic extension disrupt the generally older volcanic rocks, and those faults impinge on the eastern margin of the young arc. In the area of Butte Valley, just east of the Cascade Range north of Mount Shasta, the east margin of the topographic arc is defined structurally by east-dipping normal faults with an aggregate displacement of about 1 km, down to the east.

[1]U.S. Geological Survey.

[2]Massachusetts Institute of Technology.

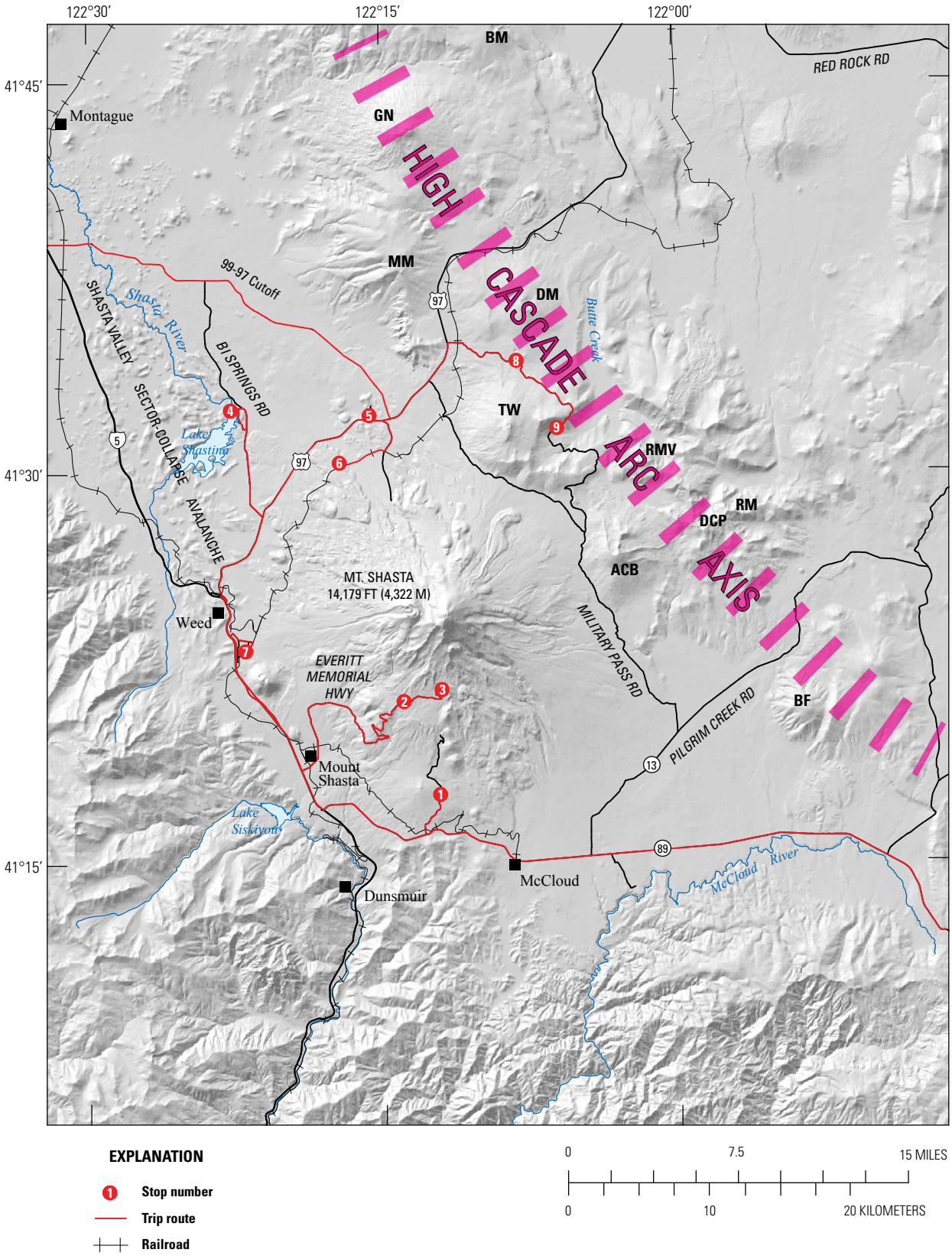

Figure 1. Digital-elevation model (DEM) and volcano-tectonic map of the Mount Shasta segment of the Cascades Arc and adjacent areas, showing place names, roads, and railroads. Field-trip route and stops in red; broken pink band is the axis of the High Cascade Arc. BM, Ball Mountain; GN, Goosenest; MM, Miller Mountain; DM, Deer Mountain; TW, The Whaleback; ACB, Ash Creek Butte; BF, Black Fox Peak; RMV, the deeply eroded Rainbow Mountain stratovolcano (with high points DCP, Dry Creek Peak; RM, Rainbow Mountain). The California-Oregon border is just north of the map near lat 42° N.

Regional Volcanism

Most of the individual volcanic edifices that define the Cascades Arc in the Shasta segment are relatively short lived shield volcanoes. In large part, these volcanoes seem to have erupted in time spans on the order of ~10^4 years. Compositions typically are basaltic andesite or andesite with SiO_2 contents of 50–60 percent. The rocks generally have moderately abundant 0.5- to 2-mm phenocrysts of plagioclase and both orthopyroxene and clinopyroxene. Olivine is a common constituent of the more mafic lavas, and the pyroxenes commonly occur as cumulocrysts, with or without plagioclase. Prominent large examples of such shields are Ash Creek Butte, The Whaleback, Deer Mountain, Miller Mountain, and Ball Mountain (fig. 1). Less common among these regional volcanoes are basaltic to basaltic-andesitic cinder-cone and lava-flow volcanoes, some of them being small monogenetic features such as Little Deer Mountain, just north of U.S. Highway 97. A few of them, however—notably Goosenest, in the northern part of the Shasta segment—are quite large and somewhat longer-lived.

Areally extensive flows of tholeiitic olivine basalt that span the age of arc activity, an altogether different type of eruptive material, are prominent in the regional volcanic suite. They range from old, deeply weathered flows, which are recognizable only by rounded residual-weathering blocks dotting the deep red soils that formed on the flows, to fresh-looking lavas of 10^5 ka or less. These lavas are typically thin, from a few meters to about 10 m in thickness, relative to their large areal extents. Although individually they are among the most voluminous eruptive units in the region, they erupted in such a highly fluid state that their vents commonly are rather inconspicuous. Where vents have been identified, they are mainly located in the vicinity of the arc axis, but the flows spread widely and mantle large areas, both along the arc axis and on its flanks. SiO_2 contents of these HAOTs are generally less than 50 percent; Al_2O_3 ranges as high as ~20 percent, and K_2O typically is less than 0.50 percent and commonly ~0.10 percent. These lavas form particularly good structural markers of the parallel normal faults related to basin-range extension, and some of them also reveal wide areas of open ground cracks.

Eruptive History of Mount Shasta

Mount Shasta, the most voluminous stratocone volcano of the Cascades Arc at about 400 km^3 (Blakely and others, 2000), is both a composite cone, in the sense of composing large proportions of both lava flows and pyroclastic and epiclastic volcanic materials, and a compound volcano, in the sense of having grown incrementally in multiple major episodes of cone building (fig. 2). The principal cone-building episodes seem to have been characterized by relatively high rates of effusive activity separated by longer periods of relatively low eruptive activity and more erosion. Plinian pyroclastic volcanism has been uncommon at Mount Shasta, although there have been a few notable plinian episodes.

Growth and Collapse of the Sand Flat Cone

The oldest lavas exposed on the Mount Shasta stratocone form a broad shoulder on the southwest side that extends from the base of the mountain to an elevation of about 2,100 m (7,000 ft). The materials exposed on this ridge are andesitic lava flows dated as ~700–350 ka ($^{40}Ar/^{39}Ar$ geochronology analyzed by USGS, Menlo Park, CA), overlain by a thin mantle of deeply weathered lithic tuffs and volcanic sediments. These volcanic materials are the principal exposed remnants of what was once a stratocone of size comparable to present-day Mount Shasta (Ui and Glicken, 1986), named the "Sand Flat cone." Most of the lavas are silicic andesites, commonly quite weathered but characterized by abundant large, strongly zoned plagioclase phenocrysts. Orthopyroxene phenocrysts commonly are replaced by oxidized Fe-oxide pseudomorphs; clinopyroxenes are less abundant than the originally hypersthenic phenocrysts. Prominent flank vents erupted andesite, dacite, and even some less common rhyodacite and low-silica rhyolite.

The Sand Flat cone may well have been the most voluminous part of the Mount Shasta edifice. The isostatic gravity field indicates that the lower parts of the edifice are depressed well below its present topographic base (Blakely and others, 2000); its volume, as estimated from both its surface and gravity expressions, may be greater than 180 km^3 although that might include at least part of its intrusive core (Blakely and others, 2000). A large fraction of the Sand Flat cone was destroyed in a massive sector collapse that produced a very large debris avalanche (fig. 3) into Shasta Valley, to the west and northwest, having a volume of about 45 km^3 (Crandell, 1989). Blocks in the avalanche resemble closely lavas of the Sand Flat cone, and ages of 666–430 ka have been obtained from some of the blocks. The tholeiitic basalt of Pluto Cave of about 116±13 ka overlies the Shasta Valley avalanche deposit, providing a minimum bracketing age of the sector collapse.

The Sargents Ridge Cone

The oldest part of Mount Shasta that postdates the Shasta Valley sector-collapse debris avalanche formed a stratocone volcano that largely healed the older collapse scar. Lavas of this edifice, named the "Sargents Ridge cone," are now exposed mainly on the south side of the mountain, on Sargents Ridge and in the valley of Mud Creek, the only deeply eroded drainage on Mount Shasta's flanks (fig. 4*A*). Sargents Ridge lavas also appear beneath younger lavas low on the west, north, and east flanks of the mountain. In places, especially in the drainage of Ash Creek on the east side, younger Sargents Ridge flows partly filled valleys that had been glacially eroded into older lavas of the Sargents Ridge cone (fig. 4*B*). The cone-building lavas range from low-silica andesite to dacite and generally have phenocrysts of plagioclase and both orthopyroxene and clinopyroxene to several millimeters diameter. Amphibole is also present in some Sargents Ridge flows. Flank vents are now exposed mainly as a group of volcanic domes and small lava cones that form a linear north-south band on the south and

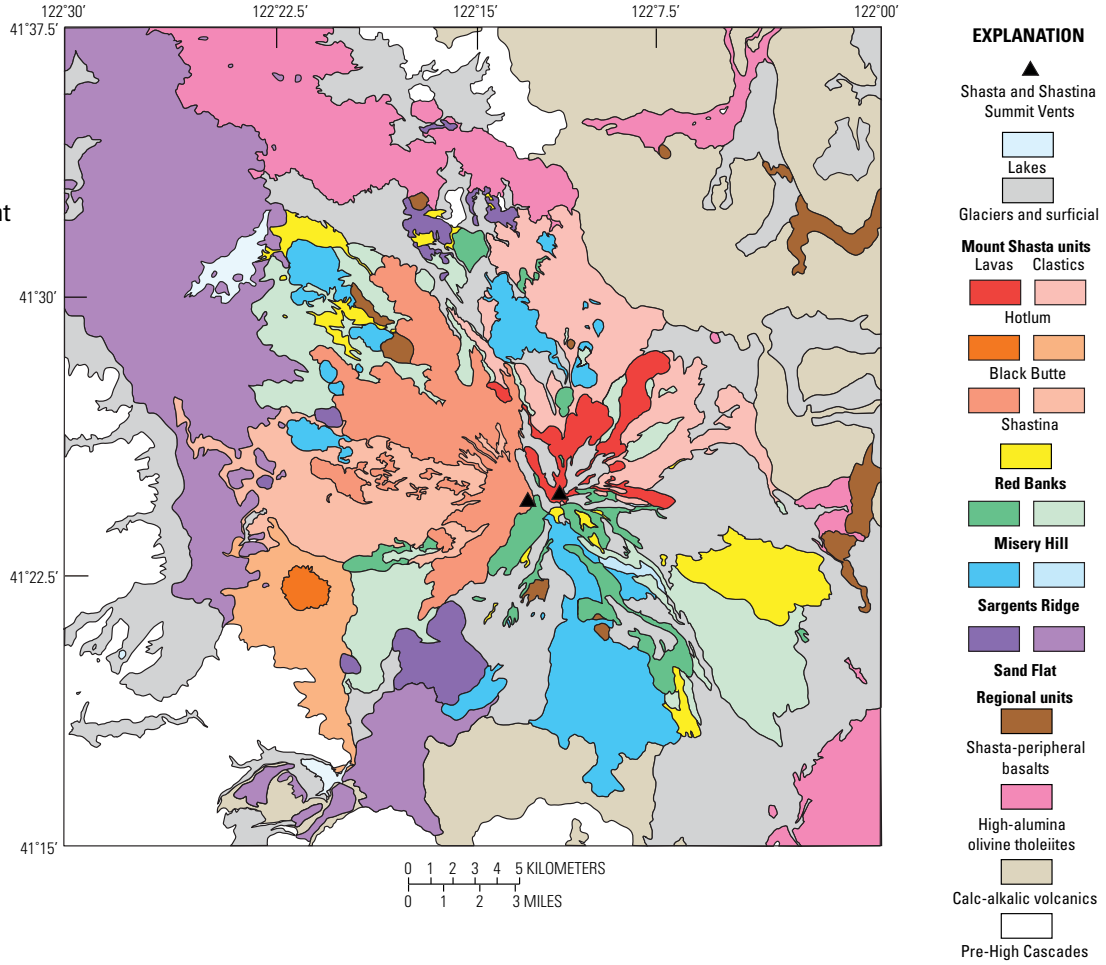

Figure 2. Simplified geologic map of the Mount Shasta stratovolcano, including its constituent cone segments and the immediately surrounding High Cascades.

Figure 3. Aerial view from the north across the Shasta Valley sector-collapse debris-avalanche deposit, with Mount Shasta and Black Butte rising in the background. The individual hills are megablocks in the avalanche, surrounded and partly mantled by laharic materials emplaced with the avalanche. The source of the avalanche is the Sand Flat cone, the oldest part of Mount Shasta, now largely buried beneath younger lavas. Photograph by J. Scurlock.

Figure 4. *A,* Aerial view from the south toward Mud Creek, Sargents Ridge (on the west side of Mud Creek), and adjacent parts of Mount Shasta. Photograph by J. Scurlock. *B*, View from the east to Ash Creek Falls, showing a younger andesite flow of the Sargents Ridge stage partly filling a valley glacially eroded into older Sargents Ridge lavas. Photograph by R. Christiansen.

north flanks, as well as in scattered localities low on the west and north sides of the volcano. Sargents Ridge lavas range in age from about 285 to about 100 ka. Some of the lower slopes of the cone contain lithic pyroclastic flows probably related to intermittent collapse events as the cone was constructed.

Because of the relatively limited extent of current exposure of Sargents Ridge lavas, it is unclear whether they represent a single, extended period of cone-building activity like the younger cone segments or perhaps several discrete episodes. Two apparent episodes are noteworthy: both the 188- to 180-ka stack of lava flows that make up Sargents Ridge itself and the 140- to 130-ka Green Butte lavas that form large ridges on the upper south flank of Mount Shasta but disappear beneath till to reappear lower on the volcano, near the City of Mount Shasta. Correlative flows floor much of Avalanche Gulch. The Sargents Ridge cone has a volume of about 85 km^3 (Blakely and others, 2000) and very likely was glaciated more than once, but most direct evidence of glaciation during or just after its growth is obscured by younger materials.

The Misery Hill Cone

The next younger major cone-building episode was growth of the Misery Hill cone from a vent just south of the present summit of Mount Shasta. Silicic andesites and dacites of the Misery Hill cone form much of the exposed bulk of Mount Shasta, burying much of the Sargents Ridge cone on the north and east sides of the mountain (figs. 4 and 5). Misery Hill lavas range in age from about 60 to about 30 ka and aggregate to a volume of about 60 km^3 (Blakely and others, 2000). Numerous flank vents, represented by volcanic domes and small lava cones, lie in the same narrow north-south zone of flank vents that formed on the Sargents Ridge cone, extending from low on the south flank, across the summit, and onto the upper north slopes. The Misery Hill cone preserves major evidence of glaciation during the time of the last glacial maximum (LGM), about 30–15 ka.

Lavas of the Misery Hill cone closely resemble the older cone-building lavas in being characterized by abundant phenocrysts of plagioclase and pyroxenes. Amphibole is prominent as a phenocryst mineral in some Misery Hill flows. Quenched inclusions of more mafic magma are especially abundant in many of the more silicic andesites and dacites of the cone and generally contain minerals of similar types to the enclosing lavas although they include some of somewhat more mafic compositions.

The last Misery Hill lava eruptions emplaced a large volcanic dome into the summit crater of the cone (fig. 6). Along with volcanic debris flows, numerous lithic pyroclastic flows mantle

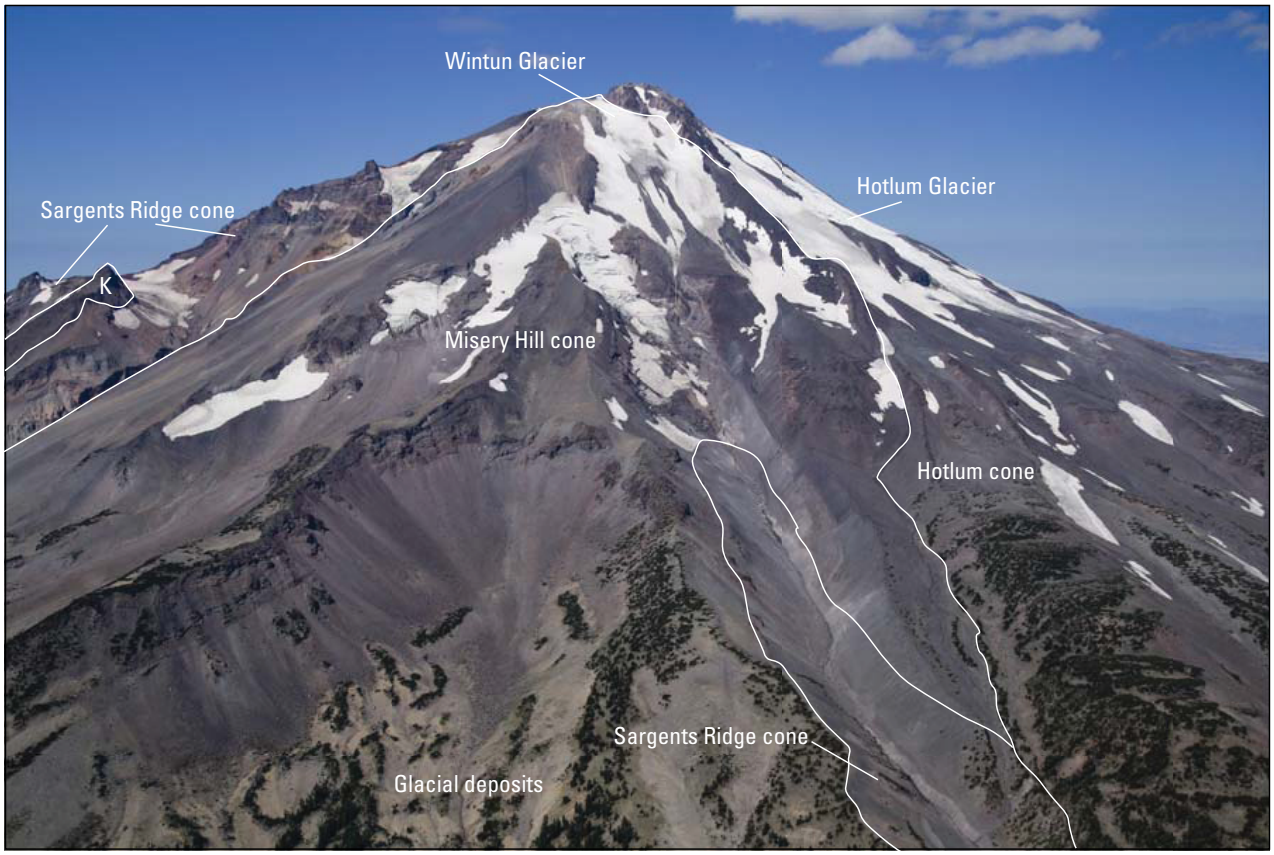

Figure 5. Aerial view from the southeast showing the Misery Hill cone and adjacent parts of Mount Shasta. The Wintun Glacier lies directly below the summit, and the Hotlum Glacier lies on the northeast slope at the right edge of the view. Sargents Ridge forms the skyline on the left. K, Konwakiton flank dome of Misery Hill age. Photograph by J. Scurlock.

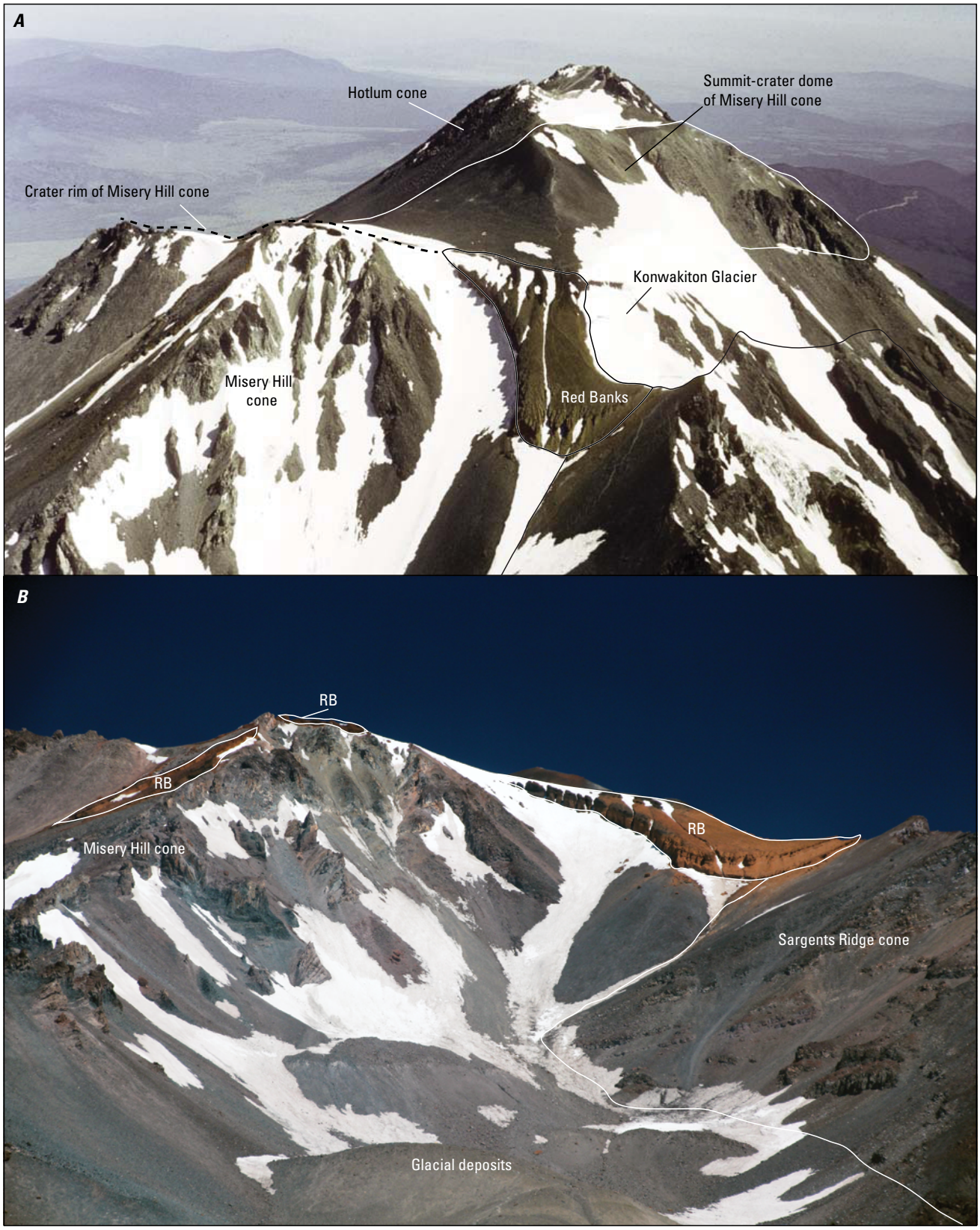

Figure 6. *A*, Aerial view from the southwest to the Mount Shasta summit, Red Banks, and a remnant of the crater rim of the Misery Hill cone. Photograph by R. Christiansen. *B,* View from the southwest up Avalanche Gulch showing erosional remnants of Red Banks pyroclastic deposits (RB) draping the Misery Hill cone and extending onto Sargents Ridge lavas at the right side of the view. Photograph by A. Calvert.

the lower slopes of the cone, typically with small to large blocks characterized by prismatic joints orthogonal to their surfaces and with pink tops to individual layers. At least some of these lithic pyroclastic deposits may reflect partial collapse events from the Misery Hill summit-dome complex.

The Red Banks Pyroclastic Eruption

The most significant pumiceous pyroclastic episode in the evolution of Mount Shasta occurred shortly after cessation of the Misery Hill cone-building episode. The Red Banks plinian eruption vented near the summit of that cone and produced andesitic to dacitic pyroclastic flows on virtually all flanks of Mount Shasta, as well as a widely distributed pyroclastic-fall blanket that extends mainly to the east and northeast. A proximal, partly agglutinated fall deposit forms a prominent feature named Red Banks just below the Mount Shasta summit (figs. 6*A*, *B*). Lavas, block-and-ash flows, and debris flows dating from each of the earlier cone-building episodes were variably mantled by pumiceous Red Banks deposits. In some sectors, especially in the drainage of Mud Creek on the south side of Mount Shasta, the pyroclastic activity generated debris flows that incorporated and became interleaved with Red Banks pumice. Much of the Red Banks pyroclastic material is conspicuously banded, with pumice having relatively less and more silicic compositions (≥57 weight percent, ≤64 weight percent SiO_2). Red Banks pyroclastic flows extended beyond the base of Mount Shasta, reaching as far west as the area of Lake Shastina (figs. 1 and 2). The thickness of the bedded pumice-fall deposit is as great as several meters on the east flank of the Misery Hill cone, and much Red Banks pumice is reworked into later deposits of lithic ash that now blanket much of the eastern sector of Mount Shasta.

The age of the Red Banks eruption, as determined by ^{14}C dating, is about 10,940 ka. It can be considered as the oldest Holocene eruption of Mount Shasta.

The Shastina Cone

Following the Red Banks episode, two further cone-building episodes built the present-day Mount Shasta edifice. The mainly older of these episodes built the Shastina cone on the west side of the mountain, and the mainly younger one forms the present summit and north and northeast flanks. There was, however, at least some overlap in these two Holocene cone-building episodes.

Perhaps the most remarkable episode in the growth of Mount Shasta occurred in the early Holocene with growth of the Shastina cone (fig. 7). This volcanic edifice, with a volume of about 15 km^3 (Gardner and others, 2013), grew entirely after the Red Banks episode at ~10,940 ka and ended

Figure 7. View from the south toward Shastina, showing its crater rim and part of a complex of partly collapsed summit domes rising within the crater. The west slope of the Misery Hill cone from the right underlies Shastina in Cascade Gulch. Photograph by R. Christiansen.

with emplacement of the Black Butte dome and pyroclastic complex at ~10,690 ka. Thus, the entire cone—one of the largest Holocene volcanic constructs in the Cascades Arc—grew entirely within a period of about 300 years or less. This extraordinary timing is confirmed by measurements of remanent paleomagnetic directions that indicate almost no secular variation during growth of the Shastina cone. Shastina formed by the accumulation of high-silica andesite and low-silica dacite lava flows that almost all erupted from a single summit vent. The lavas are lithologically generally distinct from both the older and younger lavas of Mount Shasta, especially in hosting a population of uniformly smaller plagioclase phenocrysts, generally a millimeter or less in diameter, and pyroxenes only slightly larger. Amphibole does not occur in the cone-building Shastina lavas. A single flank vent low on the north side of Shastina erupted a stack of lavas, designated as "Lava Park," identical to those from the summit vent.

Growth of the Shastina cone ended with emplacement of a series of dacite domes into its summit crater. The oldest of these domes was largely destroyed by explosive disruption and collapse to erode a narrow canyon and produce a pyroclastic-flow fan down the western flank. That event was followed by the successive emplacement of three smaller domes, each of which in turn was explosively disrupted and partly replaced by the next younger dome, generating a field of pyroclastic flows that extended more than 30 km westward to the Shasta River (figs. 1 and 2). Immediately following these dome-and-pyroclastic Shastina summit events, another dacitic dome complex formed low on Shastina's west flank. Once again, a rapid series of dacitic dome emplacements, explosive disruptions, hot avalanches, and pyroclastic flows formed the dacitic complex of Black Butte (figs. 2 and 8). The Black Butte dacites, however, are mineralogically and chemically distinct from the immediately preceding Shastina summit lavas, notably in having abundant large black amphibole phenocrysts and a lack of pyroxenes (McCanta and others, 2007).

Radiocarbon dating of pyroclastic flows, both from the Shastina summit and from Black Butte, shows that despite their clear stratigraphic distinction, all erupted within a time too short to resolve by ^{14}C dating. There was, however, a measurable change in remanent magnetic direction between the Shastina summit and the Black Butte dome and pyroclastic eruptions, suggesting that both sequences erupted within no more than about 150 years at about 10,600 ka.

The Hotlum Cone

The final stage in growth of the Mount Shasta stratocone as seen today was eruption of a sequence of silicic andesite and dacite lava flows from vents in the present summit area of the mountain, forming the Hotlum cone (fig. 9). The flows descended the north and east sides of the mountain, and some of them have been deeply gouged by the youngest glaciers, including the presently active Whitney, Bolam, Hotlum, and Wintun Glaciers. Some of the oldest Hotlum lavas erupted on

Figure 8. Photograph of Black Butte, a large dacitic flank dome; aerial view from the northeast. Four dome segments are distinguishable; the oldest is relatively low on the north (right side of the view), the youngest is the summit on the south side, the second is prominent between them, and the third is barely visible between the second and fourth dome segments. Flat valley deposits behind and in front of the domes are pyroclastic and avalanche deposits related to dome collapses. Photograph by R. Christiansen.

Figure 9. *A*, View of the Hotlum cone from the north. A remnant of the eroded Misery Hill crater rim forms the shoulder to the right of the Hotlum cone in this view. Photograph by A. Calvert. *B*, Aerial view from the east toward the Hotlum cone, showing the Hotlum Glacier, Shastina, and a small part of the eroded crater rim of the Misery Hill cone. Photograph by J. Scurlock.

the north side of the cone, and at least one of them is bracketed by young flows of the Shastina cone. Another early Hotlum flow descended the valley of Ash Creek on the east side of Mount Shasta. Lavas in both of these early Hotlum sequences have similar $^{40}Ar/^{39}Ar$ ages of about 8.5 ka and also have the same directions of paleomagnetic remanence. The youngest flows appear to have been several that erupted at the summit and were emplaced to the northeast, including the longest recognized flow, the Military Pass flow, which came within a few hundred meters of banking up against the High Cascades shield volcano of The Whaleback and the older, deeply eroded Rainbow Mountain stratovolcano.

In addition to the Hotlum lavas, much of the north and east slopes of Mount Shasta are covered by lithic pyroclastic flows from the Hotlum summit and interlayered volcanic debris flows. The last eruptive events of the Hotlum cone were numerous lithic-pyroclastic eruptions. Virtually all the deposits of these latest eruptions are strongly reworked by both wind and stream action and are now preserved as a field of well-sorted gray sand that mantles almost all the upper slopes of the mountain on the north, east, and south sides and extends well beyond the cone to the east. These sands also contain abundant fragments of pumice from fallout deposits of the Red Banks eruptions, sometimes occurring as reworked lenses or layers distributed through the sandy material. The specific vent (or vents) for these phreatic explosions is not evident, but it seems likely that the eruptions occurred from the Mount Shasta summit area. It is even possible that one such eruption occurred as recently as the late 18th century, when such an event was interpreted from observations made at sea by the explorer La Perouse in 1784 (Finch, 1930; Harris, 1988).

No associated radiocarbon has been found with the Hotlum lava flows, and, because of their young ages and the difficulty of collecting material well suited for Ar dating, knowledge of their ages is sketchy. $^{40}Ar/^{39}Ar$ ages ranging from about 10 to 0.6 ka have been obtained from several of them but with large probable errors. The total volume of these flows is >10 km^3, probably similar to that of the Shastina cone.

Parental Magmas and Petrologic Evolution of the Mount Shasta Suite

The volcanic materials erupted at Mount Shasta form a calc-alkaline suite ranging in composition from basaltic andesite to rhyolite; by far the majority of the lava flows, domes, and pyroclastic flows, however, are high-silica andesite to low-silica dacite with 60 to 67 weight percent SiO_2 (fig. 10) but with ample evidence of magma mixing. Small volumes of magmas inferred to be parental—primitive magnesian andesite (PMA), basaltic andesite (BA), and high-alumina olivine tholeiite (HAOT)—are represented by cinder cones and lava flows on the flanks of the stratovolcano and nearby (Baker and others, 1994; Bacon and others, 1997; Grove and others, 2002; Grove and others, 2003).

Mount Shasta andesites and dacites have unusually high Mg numbers (60 to 65, where Mg# = 100*Mg/(Mg+Fe*),

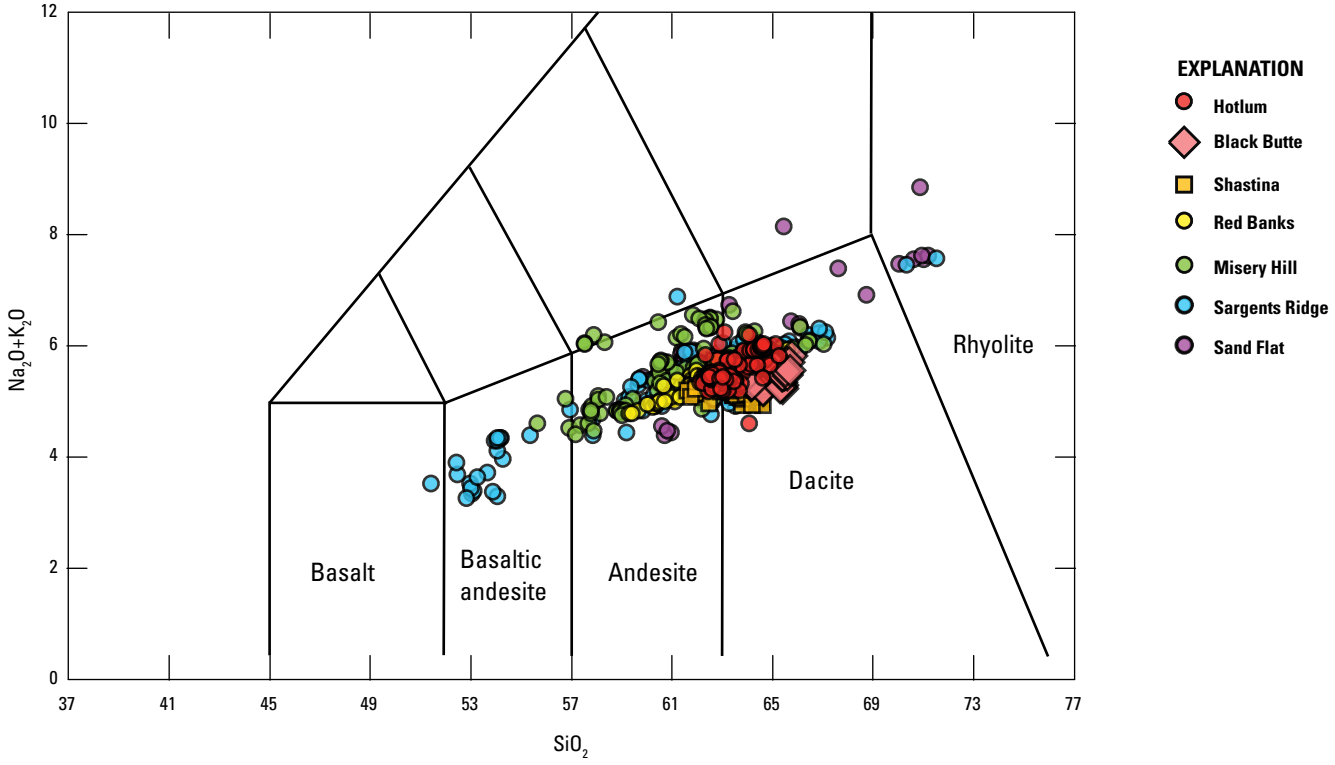

Figure 10. Plot of total alkalis vs. SiO_2 for volcanic rocks of Mount Shasta.

atomic, and Fe* is all Fe calculated as Fe^{2+}). The most primitive Mount Shasta andesites have MgO contents of 3.5 to >5 weight percent and SiO_2 contents that range from ~59 to 62 weight percent. Quenched magmatic inclusions are preserved in many Mount Shasta andesite and dacite flows and domes, some containing MgO >5 weight percent. These mafic inclusions represent more primitive magmatic inputs to the stratovolcano plumbing system, are similar to inferred parental magmas exposed regionally, and preserve evidence of the compositional characteristics and the pressure and temperature conditions of differentiation for the andesite and dacite lavas.

Figure 11 shows the compositional variations of lavas in the Mount Shasta stratocone. Alumina contents range from 16 to 18 weight percent (fig. 11*A*); there is no systematic correlation of Al_2O_3 abundance with the amount of modal plagioclase in the sampled population (Baker, 1988). Abundances of CaO (fig. 11*C*), FeO*, and TiO_2 decrease with decreasing MgO (for example, fig. 11*F*), while K_2O and Na_2O increase with decreasing MgO (figs. 11*D*, *E*). Also plotted in figure 11 are the compositions of regional lavas in the Shasta segment of the Cascade Arc—basaltic andesite and primitive magnesian andesite—interpreted as compositionally equivalent to primitive magmas.

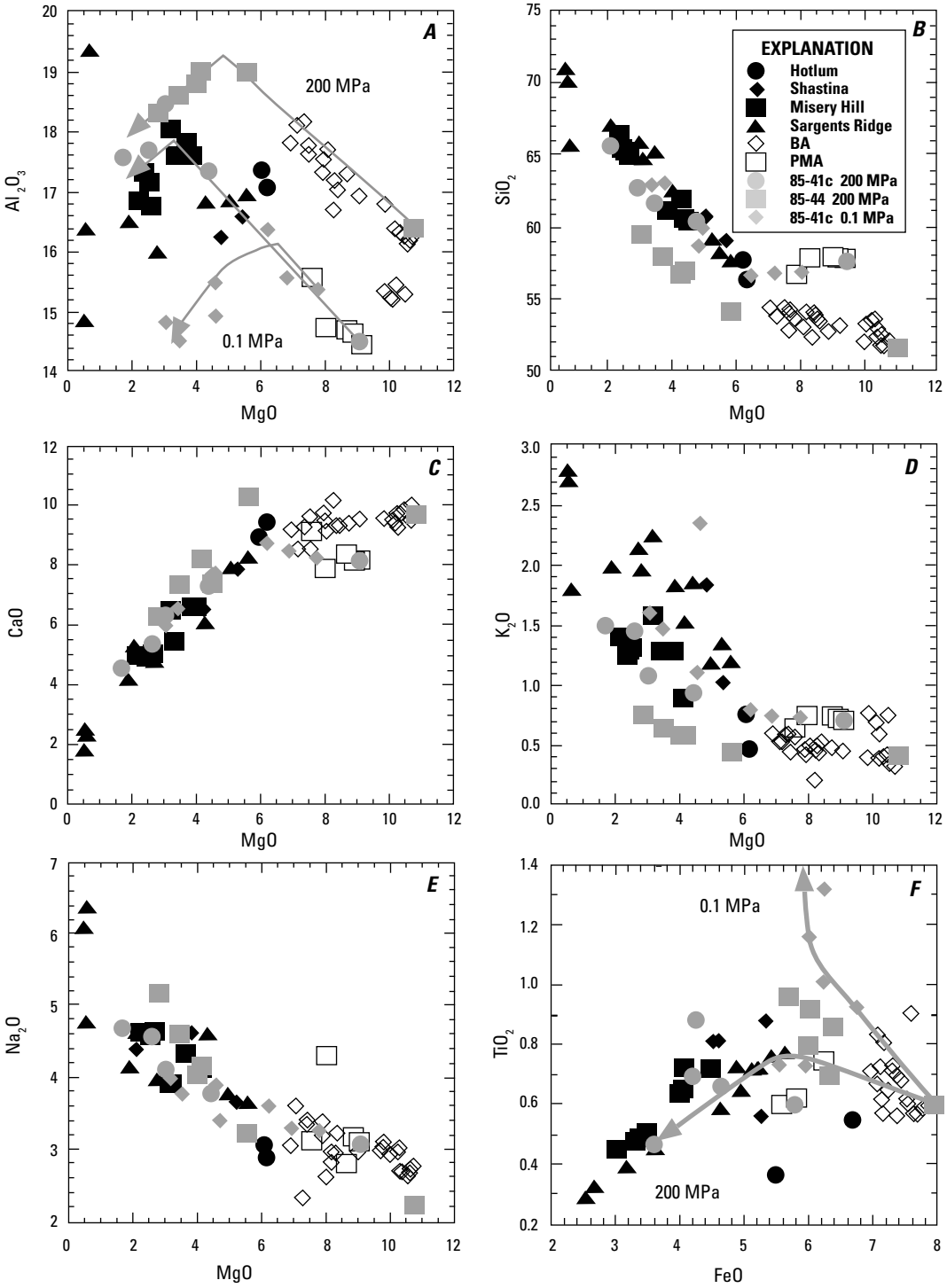

Figure 11. Major-element compositional variations in lavas of the Mount Shasta region. Also shown are compositions of basaltic andesite (BA) and primitive magnesian andesite (PMA) lavas and experimentally determined liquid lines of descent from 200-MPa, NNO-buffered, H_2O-saturated crystallization experiments on samples 85-44 and 85-41c, and 0.1-MPa QFM-buffered anhydrous experiments on 85-41c (Baker and others, 1994; Grove and others, 2002, 2003). *A*, Al_2O_3 vs. MgO, *B*, SiO_2 vs. MgO, *C*, CaO vs. MgO, *D*, K_2O vs. MgO, *E*, Na_2O vs. MgO, *F*, TiO_2 vs. FeO. FeO scale spans 2 to 8 weight percent. All oxides are in weight percent. MPa, megapascal; NNO, nickel-nickel oxide; QFM, quartz-fayalite-magnetite. Figure from Grove and others (2005).

Eruptive products are porphyritic to various degrees and contain between 2 and 40 volume percent phenocrysts (fig. 12). Most of the Mount Shasta stratocone lavas contain between 20 and 30 percent phenocrysts. All of the Mount Shasta andesites and dacites show evidence of magma mixing. Most of the stratocone lavas have been classified as plagioclase-phyric, two-pyroxene lavas, but this nomenclature belies the rich petrologic complexity present in their phenocryst assemblages. A more appropriate classification would be multi-pyroxene andesites as most Mount Shasta lavas represent multi-component mixed magmas. Furthermore, about 15 percent of the lavas contain olivine and (or) amphibole in addition to several distinct populations of plagioclase, orthopyroxene, and high-Ca clinopyroxene.

Plagioclase is the dominant phenocryst in lavas of the Sand Flat, Sargents Ridge, Misery Hill, and Hotlum cones, constituting >70 percent of the phenocryst volume. These plagioclase phenocrysts are tabular and subhedral and range from 0.5 to 5 mm in longest dimension, with <1 to 3 mm being the typical size range. Orthopyroxene, the next most abundant phenocryst phase in these lavas, is equant, elongate to irregular in shape, and 1–1.5 mm in length. Augite phenocrysts in these lavas are subhedral, equant, and <1 mm in longest dimension. Phenocrysts in Shastina lavas are generally similar in types, but the plagioclase is generally smaller and more euhedral; orthopyroxene generally predominates over clinopyroxene.

Although relatively less abundant, amphibole, olivine, and ilmenite/magnetite are also present in some of these lavas. Amphibole crystals are equant and elongate and generally range from <0.5 to ~2 mm in length. Olivine and ilmenite/magnetite range in size from 0.1 to 1 mm. Olivine crystals may have irregular or cuspate outer margins and commonly are overgrown by orthopyroxene or amphibole. Crystals of ilmenite/magnetite are subhedral, range from 0.3 to 0.8 mm in longest dimension, and commonly consist of distinct grains that share a common interface.

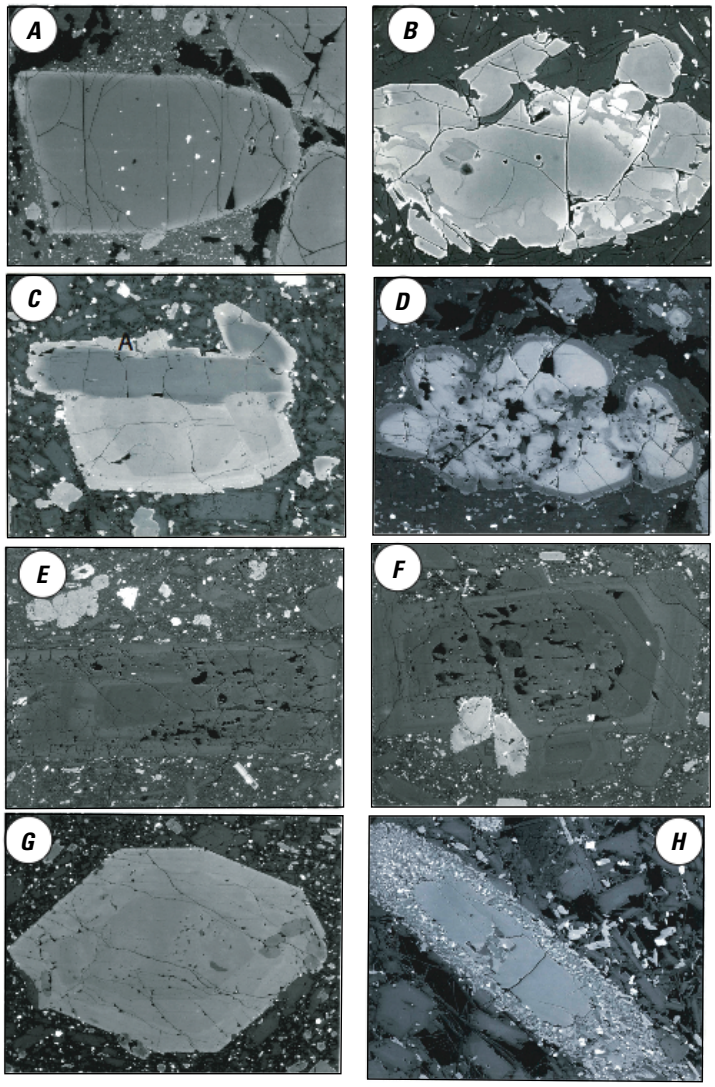

Figure 12. Phenocryst textures of andesites and dacites of the Mount Shasta region. Back-scattered electron images have a horizontal width of 0.25 mm unless otherwise noted. *A*, Fo_{90} olivine with Cr-spinel inclusions in andesite of Sargents Ridge. *B*, $Fo_{70–75}$ olivine core and Fe-rich rim overgrown by orthopyroxene in andesite of Misery Hill. *C*, Magnesian augite and orthopyroxene intergrown as glomerocrysts in andesite of Misery Hill, sample 85-48b; image width 0.1 = mm. Both augite and orthopyroxene are surrounded by distinctive Fe-rich overgrowth rims. *D*, Fe-rich orthopyroxene overgrown by Mg-rich rim, showing complex resorption/reaction texture, a characteristic of melt/xenocryst reaction; andesite of Sargents Ridge. *E*, Oscillatory zoned plagioclase phenocryst containing Ca-rich core (~An_{70}) in andesite of Misery Hill. *F*, Oscillatorily zoned plagioclase phenocryst containing Na-rich core (~An_{40}) in andesite of Sargents Ridge. *G*, Mg-rich augite (Mg# ~90) in andesite of Misery Hill. Outer, normally zoned exterior includes Mg-rich orthopyroxene (Mg# ~87). *H*, Reacted amphibole phenocryst in dacite dome of Shastina, sample 83-57; image width = 1.25 mm. Interior of the crystal contains plagioclase and orthopyroxene. Exterior rim consists of pyroxene + spinel + plagioclase reaction assemblage. Figure from Grove and others (2005).

Experimental Petrology

The compositions of olivine, orthopyroxene, augite, and amphibole with high Mg# in the Mount Shasta andesite and dacite lavas are used along with the mineral compositions produced in experiments on primitive BA and PMA liquids to identify the conditions and liquid compositions of the mafic end member(s) involved in magma mixing.

Grove and others (2003) performed 200-MPa experiments on the primitive lavas (BA and PMA). Olivine is the liquidus phase, and the most magnesian olivine in the Mount Shasta stratocone lavas falls within the range of the liquidus BA and PMA olivine compositions ($Fo_{89–93.8}$). At high H_2O contents, the first silicate mineral that crystallizes after olivine is augite. The composition of the coexisting augite and olivine can provide evidence of magmatic H_2O content. In the 200-MPa experiments, the first clinopyroxene

to crystallize has an Mg# of ~90 and would coexist with Fo_{87} olivine; this corresponds to a peak in the frequency distribution of olivine compositions in Mount Shasta lavas. Thus, we infer that one mafic end member of mixing was a liquid derived from a BA or PMA parent that had undergone a small amount of fractional crystallization—<5 percent based on modeling of experimental liquid lines of descent—at ≥200 MPa with a pre-eruptive H_2O content of ~6 weight percent.

The appearance of orthopyroxene in primitive BA and PMA compositions depends on H_2O content. The peak of orthopyroxene composition at Mg# of 85 corresponds to ~100 MPa at H_2O-saturated conditions. Augite and orthopyroxene coexist as glomerocrystic intergrowths (fig. 12*C*), indicating coprecipitation. In the most Mg-rich coexisting pairs, the orthopyroxene has an Mg# of 87, and the calculated 2-pyroxene temperature for the pair is ~1,000 °C. This combination of Mg# and temperature range requires a minimum pressure of 70 MPa.

Amphibole-phenocryst core compositions show a broad peak in their frequency distribution between Mg# 73 and 83. Krawczynski and others (2006) and Grove and others (2003) investigated the significance of this high-Mg# amphibole through a series of H_2O-saturated experiments at 200 and 800 MPa over a range of fO_2 conditions. Mg#-83 amphibole found enclosing olivine and pyroxene requires an H_2O-saturated pressure >800 MPa, and lower Mg#-77 amphibole requires a pressure of 300 MPa. Magmatic H_2O contents of ~12 weight percent are necessary to stabilize the Mg# = 83 assemblage at 800 MPa.

Plagioclase-phenocryst core compositions in Mount Shasta lavas vary in their An contents. The plagioclase compositional variations produced in the PMA and BA experiments are quite distinct. At 200 MPa the first plagioclase to crystallize in the BA is An_{82}; the first plagioclase to crystallize in the PMA is An_{72}. As H_2O-saturated pressure drops, the first plagioclase to appear in the crystallization sequence becomes less An-rich. Therefore, the interpretation of the distinct plagioclase composition in the Shastina lavas most consistent with the experimental data is that the Shastina lavas contain a mafic component similar to the PMA composition that crystallized at ~200 MPa, H_2O-saturated. The other eruptive phases of the stratocone appear to have received contributions from both an H_2O-rich BA parent and an H_2O-rich PMA parent.

Summary of Parental End-Member Magmas

The combined evidence from all the phenocryst mineral compositions (Fo_{90} olivine, Mg# 90 augite, Mg# 82 orthopyroxene, and An_{70} plagioclase) allows us to identify the dominant mafic component of the mixture of end-member components as PMA. The PMA crystallizes this mineral assemblage at 200 MPa, H_2O-saturated. Thus, a pre-eruptive H_2O content of ~6 weight percent H_2O is indicated. The minimum pressure at which this crystallization would occur should be at depths of >7 to ~9 km, or deeper if the melt was undersaturated or saturated with a mixed-volatile fluid. However, the presence of Mg-rich amphibole and high H_2O contents (10.8 weight percent) in melt inclusions (Grove and others, 2003) indicates the presence of an additional mafic component that experienced higher-pressure fractional crystallization in the lower crust at pressures as high as 900 MPa. In addition, the presence of high-An plagioclase (>An_{80}) implies the involvement of another mafic input with the composition of the BA, again at 200 MPa H_2O-saturated conditions.

Evolved End-Member Magmas

The identity of the evolved component(s) of the mixed Mount Shasta lavas cannot be inferred from the experiments carried out on the primitive Mount Shasta region lavas by Grove and others (2003). The most evolved component in the lavas appears to be a magma that was saturated with amphibole (Mg# 65–57), orthopyroxene (Mg# 55–60), plagioclase ($An_{30–40}$), and ilmenite/magnetite ± apatite. This mineral assemblage indicates the presence of a liquid that is more evolved than that found in the lowest-temperature experiments on the BA and PMA compositions, which have SiO_2 contents of ~59 weight percent and ~66 weight percent, respectively, on an anhydrous basis (Grove and others, 2003). The McKenzie Butte satellite vent to the south of the Sand Flat cone of Mount Shasta (figs. 1 and 2) is a rhyodacite (fig. 11) containing phenocrysts similar in composition to the most evolved mineral assemblage in the frequency distribution of phenocryst cores from Mount Shasta andesite and dacite lavas; it is assumed to represent one of the evolved end members of mixing. The intermediate peak in the orthopyroxene (Mg# 65–70) and plagioclase ($An_{40–50}$) compositional frequency distribution indicates a third component similar to the lowest-temperature liquid and crystal assemblage in the PMA composition, and this is assumed to represent a third component of the mixture.

Trace Element and Isotopic Variation

Grove and others (2002) characterized the trace-element and isotopic variability of Mount Shasta lavas (fig. 13). They propose that the trace elements come dominantly from a fluid-rich component derived from subducted oceanic lithosphere. They attribute the variation to contributions from different slab-derived components. One component has $^{87}Sr/^{86}Sr = 0.7028$ and $\varepsilon Nd = +8$ and is most similar to a mid-ocean-ridge basalt (MORB) source. The second component has more radiogenic $^{87}Sr/^{86}Sr = 0.7038$ and $\varepsilon Nd = +1$ (fig. 14) and is most similar to a sediment.

The fluid-rich component not only contributes the majority of the incompatible-element budget (>99 percent) but controls the Pb, Sr, and Nd isotopic composition of the lavas. Reactive porous-flow and flux melting in the mantle wedge contribute most of the major elements (>90 percent), but a significant contribution of H_2O, Na_2O, and K_2O comes from the subducted slab. The two fluid-rich components could be small-degree partial melts or supercritical hydrous fluids derived from oceanic crust and sediment.

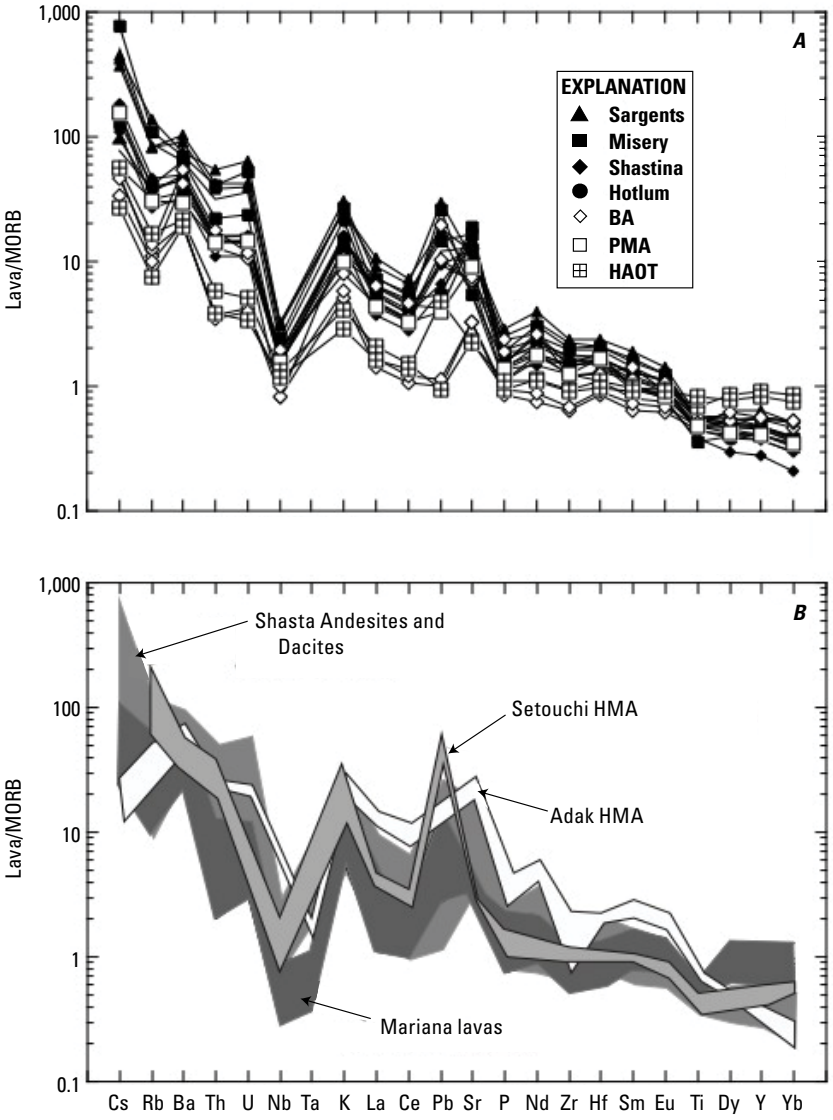

Figure 13. *A*, Mid-ocean-ridge basalt (MORB) normalized multi-element abundance diagram for selected lavas from the Mount Shasta region. *B*, Shaded fields show the range of element abundances for Mariana lavas and for high-Mg andesites from the western Aleutian arc and the southwestern Japan arc. Figure from Grove and others (2002). BA, basaltic andesite; HAOT, high-alumina magnesian andesite; HMA, high-magnesian (Mg) andesite; PMA, primitive magnesian andesite.

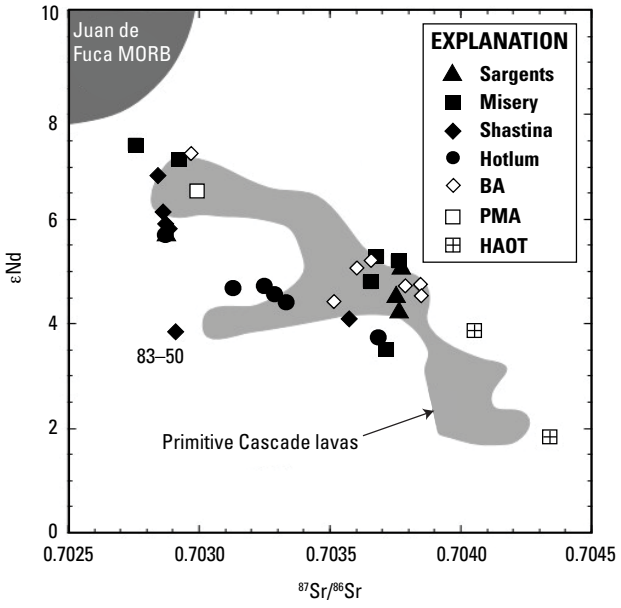

Figure 14. Values of εNd vs. $^{87}Sr/^{86}Sr$ for selected lavas from the Mount Shasta region. Only a portion of the field for Juan de Fuca MORB lavas is shown. Light-gray field outlines variation in primitive Cascade lavas from Mount Adams in southern Washington to Lassen Peak in northern California. BA, basaltic andesite; HAOT, high-alumina magnesian andesite; PMA, primitive magnesian andesite. Figure from Grove and others (2002).

Magmatic Processes

Figure 15 shows a schematic model of magmatic processes that is consistent with the existing lava- and mineral-chemical variations and that may have produced the andesite and dacite lavas of the Mount Shasta stratocone. In this model, primitive H_2O-rich mantle melts are supplied to the crustal-level magmatic system. These magmas have major-element compositions similar to PMA—high H_2O contents (4.5–6 weight percent or greater) and highly variable trace-element abundances inherited from a subduction-derived fluid-rich component. Mineral-compositional evidence suggests fractional crystallization of the primitive magmas over a great range of depths, from olivine + amphibole + pyroxene fractionation as deep as the base of the crust to olivine + pyroxene fractionation at 7 to 10 km and shallower, even to directly beneath the volcanic edifice. Lavas produced during a stratocone summit eruption sample fractionation products that formed over a broad range of depth and pressure to produce multi-component mixed magmas.

Glacial Geology

Mount Shasta, at 4,322 m (14,179 ft) elevation, is by far the highest mountain in northern California, and the part of the Cascade Arc axis between Mount Shasta and the Medicine Lake volcano is also a highland, now reaching about 2,400 m (~8,000 ft). The Rainbow Mountain volcanic center, which predates both the Mount Shasta and Medicine Lake edifices, was once a stratovolcano comparable in size to present-day Mount Shasta. Glaciers marked each of these high areas as well as high parts of the adjacent Klamath Mountains to the west, such as Mount Eddy and the Castle Peak region, through much of the Quaternary.

Five significant glaciers still mantle parts of the north and east flanks of Mount Shasta (for example, figs. 5 and 9), as well as the head of Mud Creek on the south side (fig. 4*A*). The largest modern glacier is the Whitney Glacier that occupies the north-facing declivity between the Shastina and Hotlum cones. The lower extent of its present ice is about 2,970 m (9,750 ft), but its toe is largely covered by extensive rockfall material from both sides of the glacier.

Late Holocene glaciers, including Little Ice Age advances late into the 19th century, left deposits to elevations at least as low as about 2,890 m (9,500 ft) on the north and northeast sides of Mount Shasta (fig. 9*B*) and to about 2,585 m (8,480 ft) in the valley of Ash Creek on the east side. An earlier Holocene ice advance left till deposits to elevations as low as about 1,920 m (~5,840 ft) on the east side of Mount Shasta, although younger pyroclastic-flow deposits from the Hotlum cone mantle much of

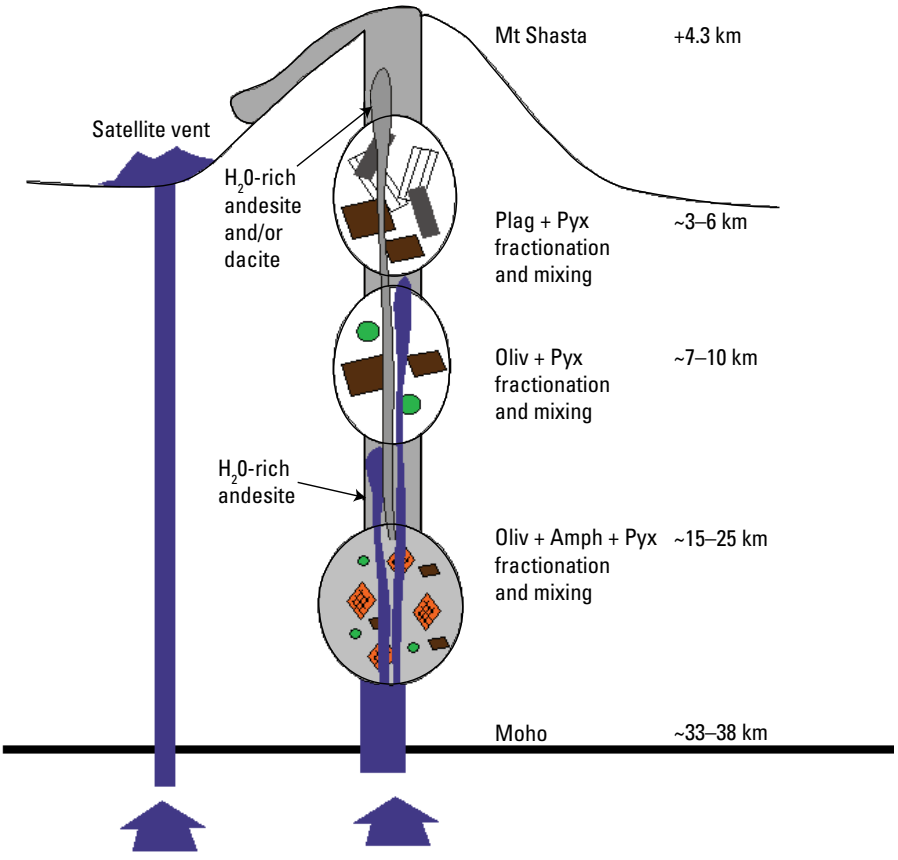

Figure 15. Schematic representation of the crustal-level fractional crystallization, magma recharge, and magma mixing processes responsible for the generation of andesites and dacites of the Shasta region. Numerous magmatic reservoirs are envisioned beneath Mount Shasta, where fractional crystallization under high H_2O contents generates andesite and dacite derivative liquids. Periodic recharge of these magma reservoirs by primitive parent magmas produces multi-component mixed andesite and dacite lavas. The parent magma for most of the Mount Shasta stratocone lavas is thought to be similar to PMA in major elements but varied in trace-element and isotopic compositions over a range spanned by all primitive lavas of the Mount Shasta region. Amph, amphibole; BA, basaltic andesite; H_2O, water; Oliv, olivine; Plag, plagioclase; PMA, primitive magnesian andesite; Pyx, pyroxene.

that till. We interpret hummocky, blocky deposits in the upper parts of several valleys on the south slope—notably in Avalanche Gulch and the old Mount Shasta ski bowl—as having been left by rock glaciers of age similar to these early Holocene glaciers on the east side.

Evidence for Pleistocene glaciation on Mount Shasta is clearest for the time of the latest major glaciation, about 30–15 ka, equivalent in age to the Tioga glaciation of the Sierra Nevada (Clark and others, 2003) or marine oxygen-isotope stage (MIS) 2 (Lisiecki and Raymo, 2005). During that glaciation, the youngest part of Mount Shasta was the Misery Hill cone, and glaciers descended all sides of the mountain to elevations as low as about 1,580 m (~5,200 ft) on the south side (for example, fig. 6*B*). It appears that the earlier ice advances during that glaciation, probably equivalent in age to the till of Raker Peak near Lassen Peak, which is bracketed by ages of 27±1 and 35±1 ka, extended to the maximum limits of the latest Pleistocene glaciation on Mount Shasta. A later major advance during that glaciation, probably equivalent to the till of Anklin Meadows at Lassen, about 17–11 ka, appears to have extended to elevations no lower than about 1,920 m (~6,300 ft).

Late Pleistocene glaciers also carved conspicuous valleys and left moraines along the higher parts of the Cascade axis east of Mount Shasta. Cirque glaciers and small valley glaciers left deposits on Ash Creek Butte, immediately to the east of Mount Shasta, and in valleys eroded into the older Rainbow Mountain stratovolcano, most notably on the sides of Dry Creek Peak, Rainbow Mountain, and Haight Mountain (fig. 1).

Little evidence of the next older major glaciation (MIS 6), which ended at about 130 ka, is found on Mount Shasta itself as deposits would have been buried by younger lavas and other deposits. Nevertheless, at least one locality, at Ash Creek Falls (fig. 4*B*), preserves clear evidence of that glaciation. There, a Sargents Ridge flow of 114.4±1.2 ka fills a U-shaped valley carved into an older flow of 172.2±1.2 ka. Further indications of a major glaciation during that time are clear in the highlands around Mount Shasta, especially near the arc-axis highlands around the Rainbow Mountain volcanic center and in the Klamath Mountains west of Mount Shasta. The outwash plain of an older glaciation that covered part of the Butte Creek drainage is marked by a conspicuous periglacial terrain of stone rings and polygons (Masson, 1949). Similar periglacial features also are preserved in the debris-flow matrix of the Shasta Valley sector-collapse avalanche deposit; soils in both of these areas of polygonal ground are similar and suggest that they relate to the same period of ice advance, possibly that of MIS 6 or perhaps even older.

A significant, even older Pleistocene glaciation produced important features of the landscape of the Mount Shasta area. Its age is not well constrained, but it clearly was the most voluminous glaciation for which evidence remains. Most significantly, much of the Rainbow Mountain stratovolcano was removed by erosion during that glaciation, now clearly recorded in the network of large U-shaped valleys that head in the core of that stratocone and descend into the valley of Butte Creek (fig. 1) to a terminus at 1,460 m (4,800 ft), where it left a terminal moraine and a significant outwash plain. Local evidence for the age of these deposits is weak. They are overlain by the extensive HAOT basalt of Pluto Cave, the $^{40}Ar/^{39}Ar$ age of which is determined with significant uncertainty to be about 150–100 ka. These features appear to record the most extensive ice advance recognized in this region, which probably occurred during MIS 16, about 631 ka (Dean and others, 2015).

Volcano-Related Hazards

A comprehensive hazard assessment of Mount Shasta has not been completed, but a few comments are in order here. Volcanism at Mount Shasta is most conspicuously characterized by its strongly episodic character. This seems to be true both on the longer-term scale of the several component cones of the compound stratovolcano and is recorded as well in individual closely spaced eruptive events, generally separated by longer intervals of quiescence. Consequently, it is to be expected that any return to eruptive activity at Mount Shasta might be followed closely by further events within relatively short periods of time. For example, the opening of a new vent, such as occurred to form the Shastina cone about 11,700 years ago, could usher in a century or more of repeated lava eruptions and even the growth of a new cone segment. Eruption and partial collapse of dacitic domes, such as those that plugged the summit craters of each of the main cones of the Mount Shasta stratovolcano, have produced extensive pyroclastic flows, both mantling the slopes of the mountain and extending down surrounding drainages as far as about 30 km.

The most likely hazardous events at Mount Shasta are always debris flows (lahars). These can be small or large and can be triggered by eruptive events, either effusive or pyroclastic, but are produced even more frequently by meteoric events. They can occur on any side of the mountain, but the most frequent and largest debris flows have occurred in the drainage of Mud Creek on the south side. A particularly damaging sequence of mudflows and floods occurred on Mud Creek in 1924 (Hill and Egenhoff, 1976), inundating large areas on the lower slopes, entering the drainage of the McCloud River, flowing into the Pit and Sacramento Rivers, and producing muddy floods as far away as San Francisco Bay. These debris flows resulted from a summer melting event after an especially warm summer that produced rapid melting of the snow cover on Mount Shasta's glaciers, an abnormal release of water from the Konwakiton Glacier high on the south side of Mount Shasta, and breakup of the glacier. A future event of similar magnitude would now probably be contained within the Shasta Lake reservoir, about 45–50 km downstream from the base of Mount Shasta, but the consequences could well affect many more people than they did in the early 20th century. Smaller but still consequential debris flows on the slopes and drainages of Mount Shasta are produced every few years by heavy rains, especially late-summer thunderstorms.

Road Log

Reading the discussion above before launching into the road log will acquaint the user with the geologic and petrologic framework and the stratigraphic terminology of the Mount Shasta area, thus providing a context for specific discussions in the road log.

Figures to the left of each paragraph are cumulative mileage for the day; bold figures at the end of each paragraph indicate mileage to the next item of the description.

Day 1—Drive from Burney to Mount Shasta

0.0 California Highway 89 (Calif. Hwy 89) crosses Pole Creek. Just beyond this crossing, the basalt of Pole Creek is well exposed in a deep roadcut on the right (north). The route from here westward to McCloud crosses five separate HAOT basalt units that become progressively younger from east to west. These tholeiite sheets provide excellent strain markers of regional normal faulting. The basalt of Dead Horse Creek (1,458±25 ka) is offset locally more than 90 m, the basalt of Pole Creek (974±12 ka) is offset as much as 90 m, the basalt of Algoma (876±14 ka) is offset as much as 60 m, the basalt of Nitwit Camp (414±8 ka) is offset more than 50 m, and the basalt of McCloud River (27±7 ka) is offset nearly 20 m. Though exposed on different faults, these offsets imply vertical motion between 0.1 and 0.7 mm/year. **2.0**

2.0 Dead Horse Summit. Deeply weathered tholeiitic basalt of Dead Horse Creek, which probably vented just northeast of Dead Horse Summit. **4.1**

6.1 View straight ahead to Mount Shasta, about 45 km (28 mi) to the west. **0.8**

6.9 Pass U.S. Forest Service Road 49 on the right (north), leading toward Medicine Lake and Red Rock Valley. **0.7**

7.6 Bartle, a roadside café and nearby former railroad siding. A small outcrop of basalt of Algoma is in the roadcut on the right. The road from here to Ash Creek Station at mile 13.9 is underlain mainly by HAOT basalt of Algoma. **2.5**

10.1 Pass the road to Stouts Meadow on the left (south). Just past here the road crosses a low fault scarp held up by outcrops of the basalt of Algoma. **1.4**

11.5 The road crosses another low fault scarp with outcrops of the basalt of Nitwit Camp. **0.9**

12.4 The road crosses another low fault scarp. **0.3**

12.7 Pass by Edson Creek Road (U.S. Forest Service Road 6) on the right (north) **0.8**

13.5 Pass the road to Cattle Camp on the left. **0.4**

13.9 Ash Creek ranger station. Just beyond here, the highway traverses a pahoehoe surface on the basalt of McCloud River, exposed intermittently in roadcut outcrops between here and the town of McCloud. **0.6**

14.5 Low roadcuts in the basalt of McCloud River. Across the road on the left (south), pass the turnout labeled "Vista Point." From here westward the road is straight and crosses gently downhill on a low-relief surface of pahoehoe lava of the basalt of McCloud River, continuing all the way to the town of McCloud at mile 23.8. **3.7**

18.2 Pass the road to Fowlers Campground on the left (south). **2.1**

20.3 Cross Mud Creek, which here channels deposits of the voluminous historic mudflow of 1924. **0.3**

20.6 Pass the intersection of Pilgrim Creek Road (U.S. Forest Service Road 13) with Calif. Hwy 89. **3.2**

23.8 Pass through the town of McCloud. **1.7**

25.5 Low roadcut exposures reveal basaltic-andesite lavas erupted from Everitt Hill, a low shield volcano of ~450 ka at the southwest base of Mount Shasta. **1.1**

26.6 The road bends slightly to the right. Beyond here, Calif. Hwy 89 passes roughly along the contact between the basaltic andesite of Everitt Hill, on the right (north), and Devonian metasedimentary rocks of the Kennett Formation, part of the eastern Klamath Mountains terrane, on the left (south). **1.7**

28.3 Talus slabs of the Kennett Formation mantle a high roadcut on the right (north). **0.3**

28.6 Turn right (north) at Snowmans Hill Summit onto a smaller paved road. From here the road climbs up the gentle slope of the Everitt Hill basaltic-andesite shield volcano in the direction of Mount Shasta. **2.1**

30.7 Pull into a large gravel parking area on the left (west) that has a maintenance shed at its far end. Park in this area.

Stop 1. View of the south flank of Mount Shasta from the east flank of Everitt Hill (fig. 16). Everitt Hill (454±31 ka) is a large monogenetic basaltic-andesite shield with lava flows that extend down

the valley of the Sacramento River more than 60 km to Lake Shasta. Looking north, volcanic domes and other vents for dacites and andesites lie along a long-lived, north-south alignment of flank vents that continues across the Mount Shasta summit. Vents are abundant along and west of this north-south alignment, but no flank vents lie to the east. The southernmost dome in this view is McKenzie Butte (464±9 ka), the most silicic (rhyodacite) eruptive unit at Mount Shasta, erupted during the pre-avalanche Sand Flat cone-building stage. Domes and flows of the Sargents Ridge, Misery Hill, Shastina, and active Hotlum cones are visible from this vantage point, as is the proximal agglutinated pumice-fall deposit of Red Banks.

Turn the vehicles around and return along the road back toward Snowmans Hill Summit. **1.1**

31.8 View straight ahead in the distance to Castle Crags, a Jurassic granitic pluton. **0.9**

32.7 Return to Calif. Hwy 89; turn right (west) toward the City of Mount Shasta. **1.8**

34.5 As the road descends the Everitt Hill basaltic-andesite shield, the view straight ahead along the road is toward Mount Eddy, a peridotite massif of early Paleozoic age in the eastern Klamath Mountains. **2.6**

37.1 After a long stretch of highway with an uphill passing lane, the road bends distinctly to the left and passes through roadcuts in very poorly sorted and deeply weathered debris-flow sediments (lahars) from the Sand Flat volcano. These cuts are now densely overgrown with shrubs of manzanita and are no longer well exposed. **0.8**

Figure 16. View from Stop 1 near Snowmans Hill Summit, looking northward toward Mount Shasta and showing the Sargents Ridge, Misery Hill, and Shastina cones, as well as the thin Red Banks pumice and scoria agglutinate deposit. The Mount Shasta summit, just visible at the top edge of the view is the only part of the Hotlum cone visible from this point. Photograph by A. Calvert.

37.9 Merge right onto Interstate 5 north. The road descends from the Everitt Hill shield onto valley sediments of both Pleistocene and Holocene ages. Mount Eddy remains clearly visible ahead on the left. **0.6**

38.5 Straight ahead is an excellent view of Black Butte, a dacitic dome complex near the west base of Mount Shasta. To its right is the lower Spring Hill, an older dome of adakitic andesite. **1.3**

39.8 Take Exit 738 on the right to the central part of the City of Mount Shasta. Exit the freeway, merging right onto West Lake Street and continuing through the City of Mount Shasta to the end of Lake Street, where a slight left bend leads onto North Washington Drive. **0.6**

40.4 At the traffic light, the road straight ahead becomes Everitt Memorial Highway and climbs gradually over young debris-flow deposits from Mount Shasta. **2.7**

43.1 Pass the dirt Black Butte Road on the left. From near here, the road bends right and climbs more steeply across lithic pyroclastic-flow deposits of the Misery Hill cone. **2.2**

45.3 The road begins to climb the forested Sand Flat volcano. **1.3**

46.6 Pass prominent outcrops of Sand Flat lavas on the left, just before a prominent bend to the left (east). Farther on, the road continues through two hairpin turns. Lavas exposed in roadcuts all along this stretch of road range from 500 to 700 ka, and deeply weathered volcanic sediments overlie the andesite flows in many of the outcrops. **3.8**

50.4 Around a sharp turn to the left, the road crosses onto part of Sand Flat, an area here characterized by an open forest of mature Shasta red fir, an endemic tree subspecies. The terrain here is underlain by ground moraine related to an early phase of the last major glaciation. **0.4**

50.8 Dirt road on the left is the west end of a loop, leading to the main part of Sand Flat. Although there is a better view of the Mount Shasta summit from there than at Stop 2, we proceed on the paved road toward Bunny Flat, where there are restrooms, as well as a suitable viewpoint. (Users of this guide may want to take the loop into Sand Flat proper at another time.) **0.3**

51.1 The road approaches the base of a ridge on the left (north). This is the terminus of the latest ice advance of the last glacial maximum (LGM), probably about 17 ka. Just beyond, the road crosses and then traverses along the base of a prominent medial moraine that was left between LGM glaciers in Cascade Gulch (on the west) and Avalanche Gulch (on the east). **0.3**

51.4 Pass the east end of the Sand Flat dirt loop road on the left. Ahead, as the road continues alongside the moraine, views to the right show the north-south alignment of flank vents related to the Sand Flat, Sargents Ridge, and Misery Hill cone-building episodes (fig. 2). In the distance to the south, Lassen Peak and its surroundings are generally visible from the road just beyond here. **0.8**

52.2 **Stop 2. Bunny Flat, elevation 6,950 ft (fig. 17).** View up Avalanche Gulch. Restrooms are available, as well as the trailhead for the main climbing route to the Mount Shasta summit. Lavas forming the southeast side of Avalanche Gulch erupted during the Sargents Ridge stage; lavas on the skyline ridge (Sargents Ridge itself) range from 182 ka to 125 ka (Thumb Rock). Lavas on the northwest side of Avalanche Gulch (Casaval Ridge) erupted during Misery Hill time. The 53–40 ka Casaval Ridge lavas may have erupted when glaciers filled Avalanche Gulch to the east and Hidden Valley-Cascade Gulch to the west as the lava margins are commonly chilled and flows are restricted to ridgelines. Red Banks (10.9 ka), a deposit of agglutinated pumice fall, drapes the headwall of Avalanche Gulch.

Continue up Everitt Memorial Highway to the end of the road at the old ski bowl, along the way traversing mainly ground-moraine deposits but also scattered outcrops of andesite-dacite lavas related to the Sargents Ridge and Misery Hill episodes. Near the end of the road are thick sandy deposits probably representing reworked lithic ash from late phreatic summit eruptions. **2.8**

55.0 **Stop 3. Old ski bowl, elevation ~7,800 ft (fig. 18).** Sargents Ridge lavas toward the summit and to the east are 188–182 ka silicic andesite lava flows. Vent-proximal scoria and lava flows form erosional spires in the core of the old Sargents Ridge volcano at the top of the ridge. Green Butte on the west valley wall is a 135-ka, Mg-rich basaltic andesite. Both the Sargents Ridge and Green Butte lavas disappear downslope beneath glacial deposits, then reemerge on the lower slopes closer to the City of Mount Shasta. The glacial valley of the old ski bowl contained a post-LGM glacier that left rock-glacier deposits on the valley floor.

From the east end of the parking lot, walk ~1 km up a marked trail toward The Gate. Upon reaching the wilderness boundary sign, look ahead, eastward, at Red Butte, a 20-ka andesite dome erupted along the north-south vent alignment. Red Butte and an apparently coeval lava flow in the Mud Creek cirque erupted onto LGM glacial ice at least 20 m thick at Red Butte and substantially thicker above.

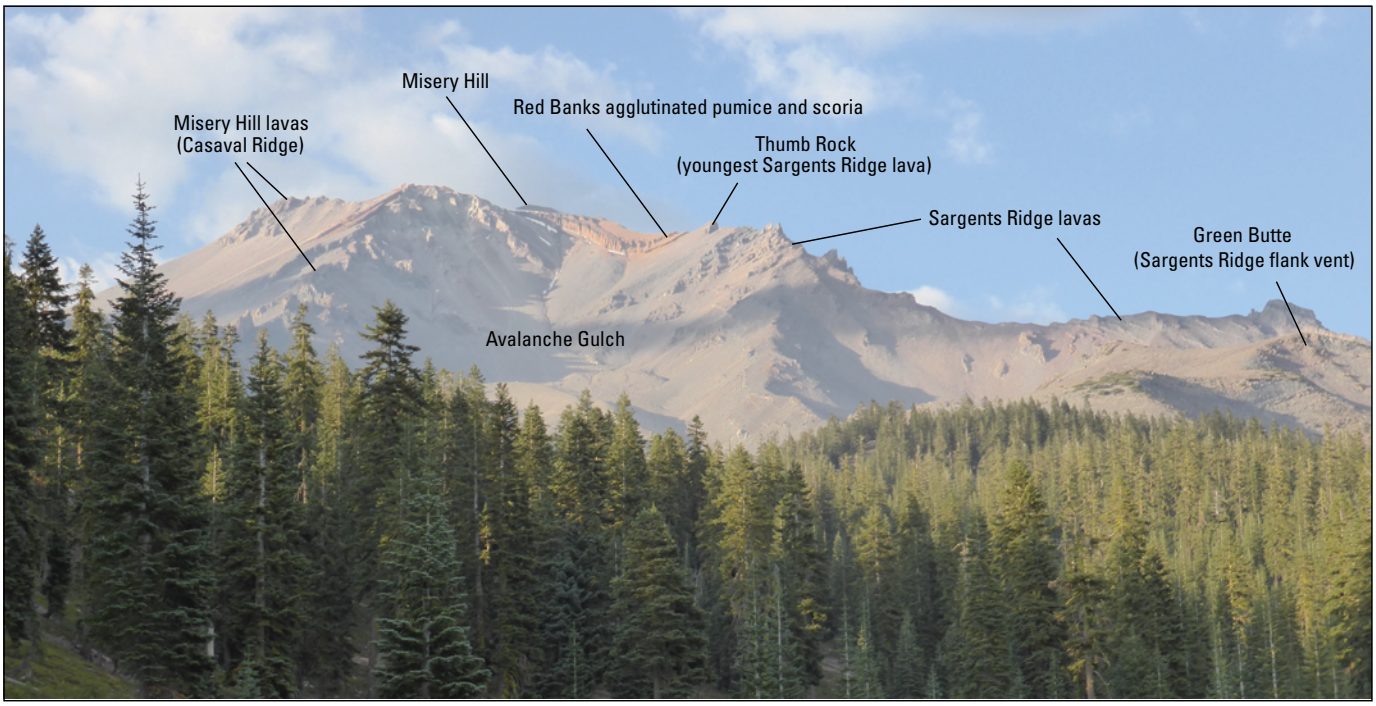

Figure 17. View from Stop 2 at Bunny Flat, looking northeastward toward the Mount Shasta summit area and showing the Sargents Ridge and Misery Hill cones. The much eroded Sargents Ridge cone is delineated by a sequence of lava flows on Sargents Ridge itself, dipping to the right (south) and on the ridge leading up to Thumb Rock, dipping to the left (north). The Misery Hill cone too is glaciated, notably in Avalanche Gulch, but less degraded than the Sargents Ridge cone; Misery Hill itself is a crater-filling summit dome of the cone. The Red Banks agglutinated pumice and scoria deposit lies atop the cirque between the two cones. Photograph by A. Calvert.

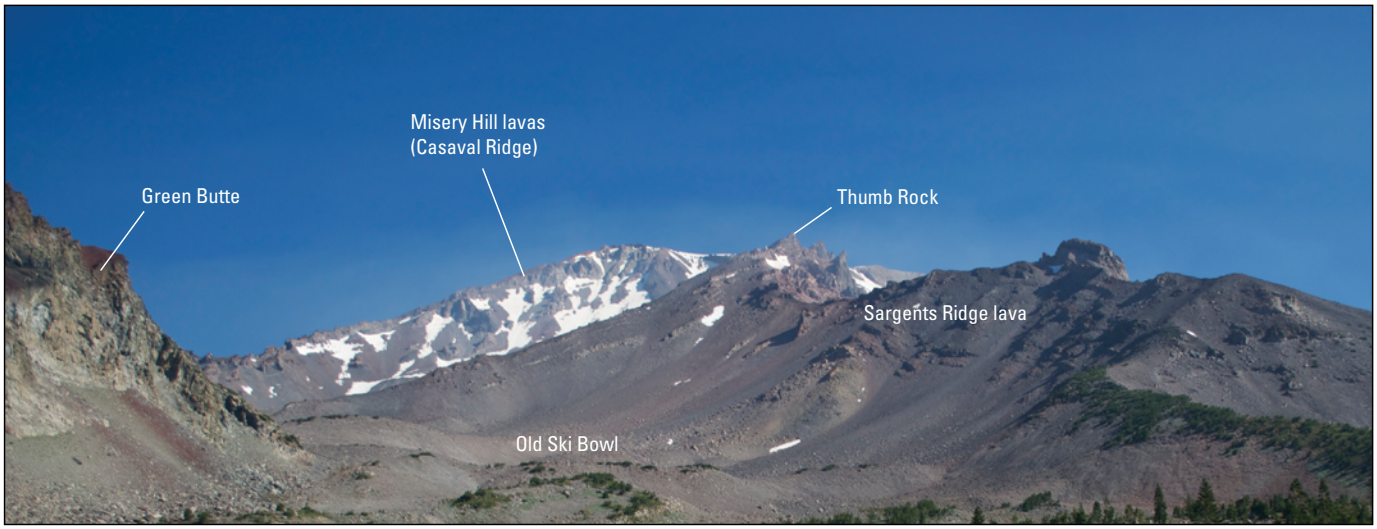

Figure 18. View from Stop 3 in the old Shasta ski bowl. The view northward is dominated by Sargents Ridge, the main exposure of the Sargents Ridge cone; at its head Thumb Rock stands at the cirque rim of the Konwakiton Glacier, which is hidden from view. Casaval Ridge is a glaciated exposure of Misery Hill lavas that may have been emplaced in Avalanche Gulch during the last glacial maximum (LGM). Green Butte is an Mg-rich basaltic-andesite flank vent the same age as the Sargents Ridge cone. The hummocky floor of the old ski bowl is formed by rock-glacier deposits left in this valley by a post-LGM glacier. Photograph by A. Calvert.

Turn the vehicles around, and retrace the route, descending Everitt Memorial Highway back toward the City of Mount Shasta. **2.8**

57.8 Pass Bunny Flat. Beyond here in distant views to the west, the Klamath Mountains can be seen, including the far distant Trinity Alps. Nearer, at the west base of Mount Shasta, are excellent views of the Black Butte dome complex. **10.7**

68.5 After returning down the slopes of Mount Shasta nearly to the City of Mount Shasta, turn right on Ski Village Drive. **0.9**

69.4 Turn right on North Mount Shasta Boulevard. Drive past Spring Hill, a 350-ka adakitic andesite cone. A large spring below the road on the south edge of Spring Hill forms part of the headwaters of the Sacramento River. **0.4**

69.8 Merge right onto Interstate 5 north. Drive past the ~1 km^3 Black Butte, a compound dacite dome erupted at the end of the ~10,700-year-old Shastina eruptive episode (fig. 8). Pyroclastic flows and deposits of hot avalanches related to Black Butte cover the valley floor here, some of which will be visited later, at Stop 7. Numerous megablocks of the Shasta Valley sector-collapse debris avalanche that destroyed much of the Sand Flat volcano line the west side of the freeway from Black Butte northward. **3.2**

73.0 Pass Truck Village on the right (east). **2.1**

75.1 Pass the highway exit to South Weed (gas stations and restaurants) and continue north on Interstate 5. The low-relief hills along the highway behind South Weed are all related to eruptive and collapse events of the Black Butte dome complex. The low areas ahead, between the Shasta Valley avalanche megablocks, are pyroclastic-flow deposits related to late summit eruptions from Shastina, which rises prominently to the east. **1.7**

76.8 Take Exit 747 toward U.S. Hwy 97. **0.3**

77.1 Turn right into the town of Weed. **0.4**

77.5 At the second traffic light, merge right onto U.S. Hwy 97 and continue through the outer parts of Weed and its outskirts. All along the road, both in roadcuts and as isolated nearby rounded hills, are blocks of the Shasta Valley debris avalanche. Pass the old Weed lumber mill to the right (south). Good views of Mount Shasta to the east. **3.3**

80.8 U.S. Hwy 97 passes into a broad open valley. To the left (northwest) are hills related to the Shasta Valley debris avalanche; ahead to the right (northeast) are some dacitic flank domes related to the Sand Flat and Sargents Ridge episodes, with low-silica dacite flows of the Shastina cone partially overriding some of them. The relatively flat valley floor is underlain by a pyroclastic-flow fan related to the Misery Hill cone. **1.1**

81.9 Turn left onto Big Springs Road. Near the intersection, a Shastina flow is prominent, across U.S. Hwy 97 to the right; the conspicuous hill just north, on the right after turning onto Big Springs Road, is a megablock of the Shasta Valley sector-collapse avalanche. The road continues along the surface of a Misery Hill pyroclastic-flow fan with distant views to the northeast toward a line of basaltic-andesite shield volcanoes and cinder cones that form the crest of the High Cascade axis. **3.1**

85.0 At the end of a long straightaway and a golf course on the left (west), just before the road enters some sparsely timbered hills, the end of a thick andesitic lava flow rises on the right above the pyroclastic-flow surface. This flow, undated but related to the Sargents Ridge eruptive episode, here overlies the Shasta Valley debris avalanche deposit, which forms the low hills to the left of the road (west). **1.1**

86.1 Turn left onto Lake Shore Drive at the landscaped entrance marked "Lake Shastina." **0.2**

86.3 At the intersection with a way stop sign, turn right and continue to the hill crest. **0.9**

87.2 Park alongside the left (west) side of the road across from the intersection with Dwinnell Road. Walk west along a gravel road, across the Lake Shastina dam, to a quarry on the west side of Lake Shastina.

Stop 4. Quarry in Shasta Valley avalanche block (fig. 19). Debris avalanche megablocks litter Shasta Valley as far as 50 km from present Mount Shasta. The intervening spaces between blocks are underlain by a laharic matrix facies that also partly mantles many of the blocks. Dated lavas in some of the blocks range in age from 666 to 428 ka. This sector-collapse avalanche, with a volume of about 50 km^3, destroyed much of the Sand Flat volcanic edifice, which was later largely replaced by the Sargents Ridge volcano. The avalanche occurred sometime between 428 and 291 ka, bracketed by the youngest date on a lava block contained in the debris avalanche and the oldest dated Sargents Ridge lava flow. The quarry, which was excavated for the material in the dam, exposes the internal features

Figure 19. Stop 4, the Lake Shastina dam quarry in a megablock of the Shasta Valley sector-collapse debris-avalanche deposit. The internal structure of this relatively proximal block shows it to be broken and disturbed but, nevertheless, preserving internal stratigraphy quite well. Photograph by A. Calvert.

of a representative proximal avalanche megablock. Fragmental stratigraphy is disrupted at a small scale but is nevertheless largely intact on a larger scale, despite transport of at least 20 km during the enormous debris avalanche.

Return to the parked vehicles. Proceed north on Lake Shore Drive to Big Springs Road. **0.3**

87.5 At the stop sign, the view ahead (east) is across an open valley floored by runout of young debris flows from Mount Shasta. In the distance, are volcanoes of the High Cascades axis; a relatively rough-looking edifice slightly left of the lowest part of the skyline is a sequence of volcanic breccias that are the southernmost outcrop of Western Cascades volcanic rocks. Turn right (south) and drive back to U.S. Hwy 97. **5.3**

92.8 Turn left onto U.S. Hwy 97 and proceed northeastward, clockwise around the north side of Mount Shasta. Just past the intersection of Big Springs Road and U.S. Hwy 97, the highway passes between a Shasta Valley avalanche megablock on the left (northwest) and a Shastina high-silica andesite flow on the right (southeast). Beyond, the road crosses a Misery Hill pyroclastic-flow fan, locally but inconspicuously overlain by Red Banks pumice and, to the south, more obviously by Shastina lava flows. Ahead and somewhat to the right (southeast) is Cinder Cone, a prominent basaltic-andesite flank vent. **2.0**

94.8 The road passes from the open terrain on Misery Hill pyroclastic flows through a timbered area and some roadside outcrops of the same Sargents Ridge andesite flow that overlies the Shasta Valley avalanche deposit near Lake Shastina. Just beyond, a roadcut on the right exposes a basaltic andesite flow from Cinder Cone. **2.1**

96.9 On the right, the road passes near the conspicuous front of a blocky lava flow from a flank vent on the north side of Shastina. We will examine this flow in a well-exposed railroad cut at a later stop (Stop 6). As the road bends around this flow near its frontal scarp, it passes onto Holocene debris-flow deposits in the drainage of Whitney Creek. We cross Whitney Creek at the east side of this debris-flow field and rise onto an irregular terrain of andesitic lava flows of the Sand Flat edifice, overlain locally by Red Banks pumice and Holocene debris flows. The prominent hill to the left (north) of U.S. Hwy 97 is the 375-ka Haystack adakitic dacite dome. Just past Haystack, the highway crests, bends to the right, and begins a descent. **2.6**

99.5 At the bottom of that descent, where an east-heading passing lane starts, is a rather inconspicuous gate and a dirt road leading to the left (north); carefully cross the highway to this gate. Proceed through the gate (this is on public property, but be sure to close the gate behind the last vehicle that passes through). Drive a short distance

up the rough dirt track to a topographic saddle where the track forks and park. **0.4**

99.9 **Stop 5. Yellow Butte (fig. 20)**. Yellow Butte is the northeasternmost exposure of Klamath Mountains basement terrane. Here, schist and quartzite of the Pickett Peak terrane are intruded by a 138-Ma monzodiorite pluton. Views southward of parts of the Sargents Ridge, Misery Hill, Shastina, and Hotlum cones are excellent. Three glaciers are visible from here: Whitney Glacier lies between the main edifice of Mount Shasta and Shastina, Bolam Glacier is north-northwest of the summit, and Hotlum Glacier flows northeast from the summit. Whitney Glacier is armored by rockfall from Shastina and, unlike all other Mount Shasta glaciers, has not receded appreciably since the 1960s. Low forested hills in the middle distance are 100-ka andesite lavas of the Sargents Ridge cone and the 100-ka North Gate dacite dome. The high ridge north and northwest of the summit comprises 20- to 11-ka domes, belonging to the Misery Hill stage, along the north-south vent alignment that passes through the summit. Shastina domes and lava flows to the right of Whitney Glacier are 10,700 years old, and the higher glaciated flows to the left (east) of the glacier erupted during the Holocene Hotlum episode. Looking at the view farther around to the right (west), the dacitic Haystack dome and an older basaltic-andesite cinder cone, quarried for the cinders, are notable in the middle distance. Beyond, hillocks of the Shasta Valley avalanche deposit floor the valley, and the Klamath Mountains rise behind. **0.3**

100.2 Return down the dirt track to the gate; be sure to close it again when all cars are through, then turn left onto U.S. Hwy 97. **0.4**

100.6 The highway crosses Holocene debris flows. On the right is the front of a Sargents Ridge andesite flow; to the left,

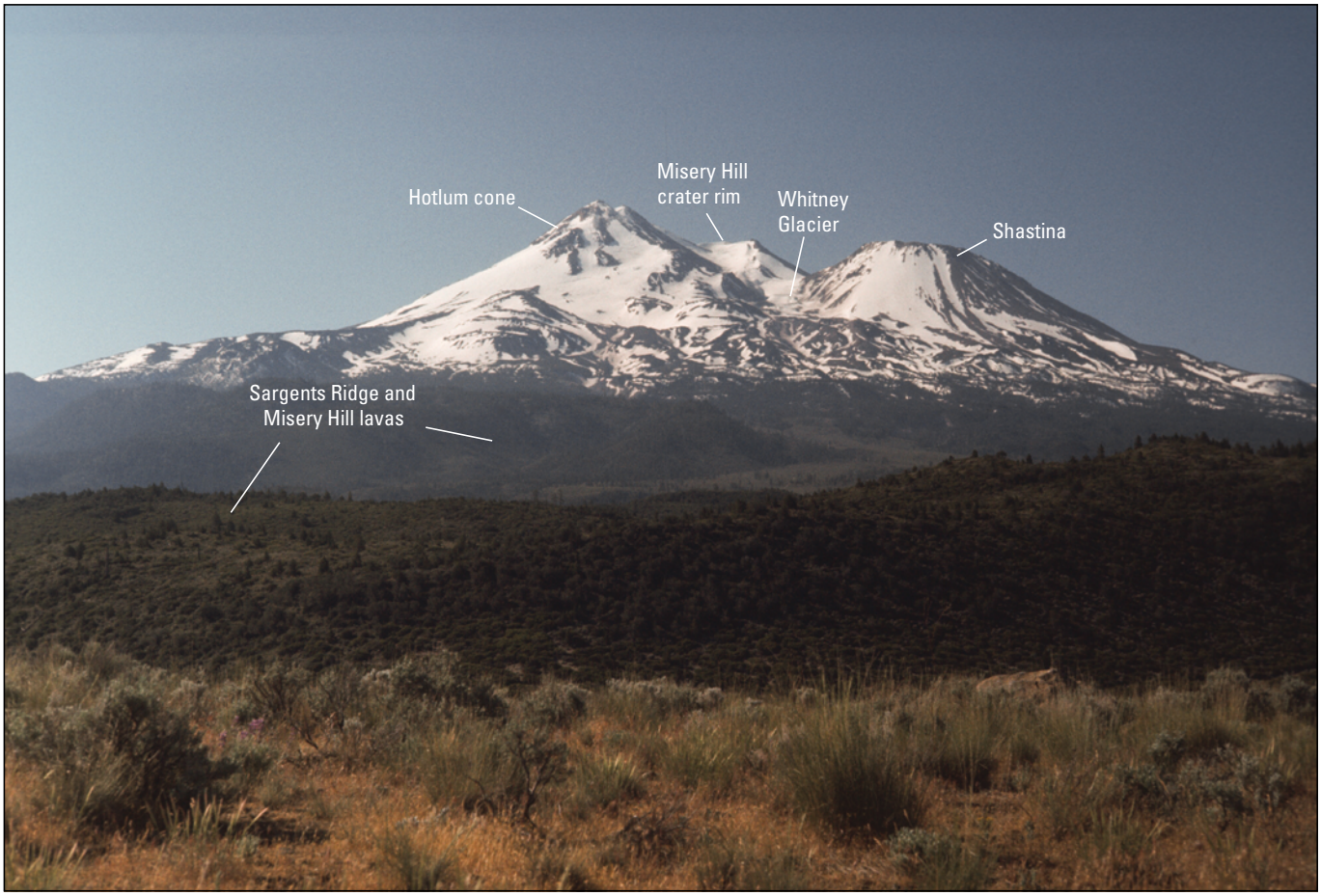

Figure 20. View to the south from Stop 5 at Yellow Butte, looking toward Mount Shasta. The Hotlum cone forms the major feature rising to the summit of the mountain; the Shastina cone, mainly just slightly older, is prominent on the right (west); the Whitney Glacier lies between these two main features, with a remnant of the Misery Hill crater rim rising above the cirque at its head. The forested slopes in the middle ground are underlain by lavas of the Sargents Ridge cone that emerge from beneath covering lavas of the younger cones. Photograph by A. Calvert.

east of Yellow Butte, are hills of a Sand Flat andesite flow. Turn right onto the gravel road, Bolam Road (U.S. Forest Service Road 43N21). **0.4**

101.0 To the right (west) of this road that courses up a gravel wash is a 100-ka Sargents Ridge andesite flow. The low hills to the left (east) are underlain by Holocene pyroclastic flows from the Hotlum cone. **1.7**

102.7 Cross the railroad tracks near the Bolam Creek Siding and turn right onto the graded right-of-way immediately alongside the Union Pacific Railroad tracks. **1.3**

104.0 The vehicles ford Whitney Creek. Subglacial outburst floods occur every few years around the volcano, particularly on hot summer days or due to heavy summer rainfall. Whitney Creek here drains both the Whitney and Bolam glaciers. A large debris flow followed heavy rains higher on Mount Shasta in August, 1997, and closed U.S. Hwy 97 downstream from here. Debris flows from Mud Creek and Inconstance Creek on the south and east sides of Mount Shasta in late summer, 2014, similarly resulted from sudden releases of subglacial water during hot weather. Park at the edge of the Lava Park andesite flow. **0.8**

104.8 **Stop 6. Lava Park flow and Whitney Creek debris flows (fig. 21)**. The Lava Park lava flow erupted from a flank vent 8 km north of Shastina and is a typical Shastina lava flow. In contrast to lavas from all other eruptive stages, Shastina lavas contain far smaller and fewer phenocrysts (5–10 percent) and have unusual trace-element contents (notably high Sr and light rare-earth element [LREE]). Walk through the flow levee and look at the rubbly block-lava surface. Views to the northwest clearly show the Shasta Valley debris avalanche. Watch out for trains; this is an active main-line track.

Turn around and return toward the crossing at Bolam Creek Siding. **2.0**

106.8 Turn left and cross the tracks onto the gravel Bolam Creek Road. **1.6**

108.4 Turn left onto U.S. Hwy 97, and continue back to Weed. **12.0**

120.4 Merge left at the traffic light onto Weed Boulevard. **0.5**

120.9 Merge left onto the Interstate 5 southbound ramp, and follow Interstate 5 south toward the City of Mount Shasta. **1.3**

122.2 Take Exit 745 for South Weed and turn left onto Vista Drive. **0.6**

122.8 At the stop sign, turn right onto Black Butte Drive (paved). **0.3**

123.1 Turn left on Black Butte Road (gravel). **0.7**

123.8 At the railroad tracks, turn right and follow the gravel roadway along the right (west) side of the tracks. Black Butte rises straight ahead. **0.4**

124.2 **Stop 7. Black Butte siding (fig. 22)**. Pyroclastic flow deposits from Shastina and Black Butte are exposed in sequence in the railroad cut. Shastina blocks contain small phenocrysts of orthopyroxene, clinopyroxene, hornblende, and plagioclase. Black Butte deposits contain phenocrysts only of black acicular hornblende and relatively minor plagioclase. Although both pyroclastic deposits are preserved here in sequence, paleomagnetic measurements demonstrate that the entire section has been distorted as a gross structural unit by slumping of the Black Butte pyroclastic complex.

Turn the vehicles around and drive back toward Black Butte Road. **0.4**

124.6 Turn left onto Black Butte Road, and return back toward South Weed. **0.7**

125.3 Turn right onto the paved Black Butte Drive. **0.3**

125.6 At the stop sign, turn left onto Vista Drive. **0.3**

125.9 Merge left onto Interstate 5 south toward the City of Mount Shasta. **6.8**

132.7 Take Exit 738 to central Mount Shasta. At the intersection, turn left. **0.5**

133.2 Just across the overpass bridge, turn right into the Tree House Motel parking lot.

Figure 21. Photos for Stop 6, the Lava Park flow from a flank vent of Shastina. *A*, Aerial view looking southeastward across the Lava Park flow toward the base of Mount Shasta; the steep flow fronts of this high-silica-andesite block-lava flow rise conspicuously above the underlying surface of a pyroclastic-flow fan of the Misery Hill cone. *B*, View toward the northwest across the surface of the Lava Park flow from its vent plug. The Shasta Valley avalanche lies below, with Lake Shastina in the left middle ground; the Klamath Mountains rise in the distance below the clouds.

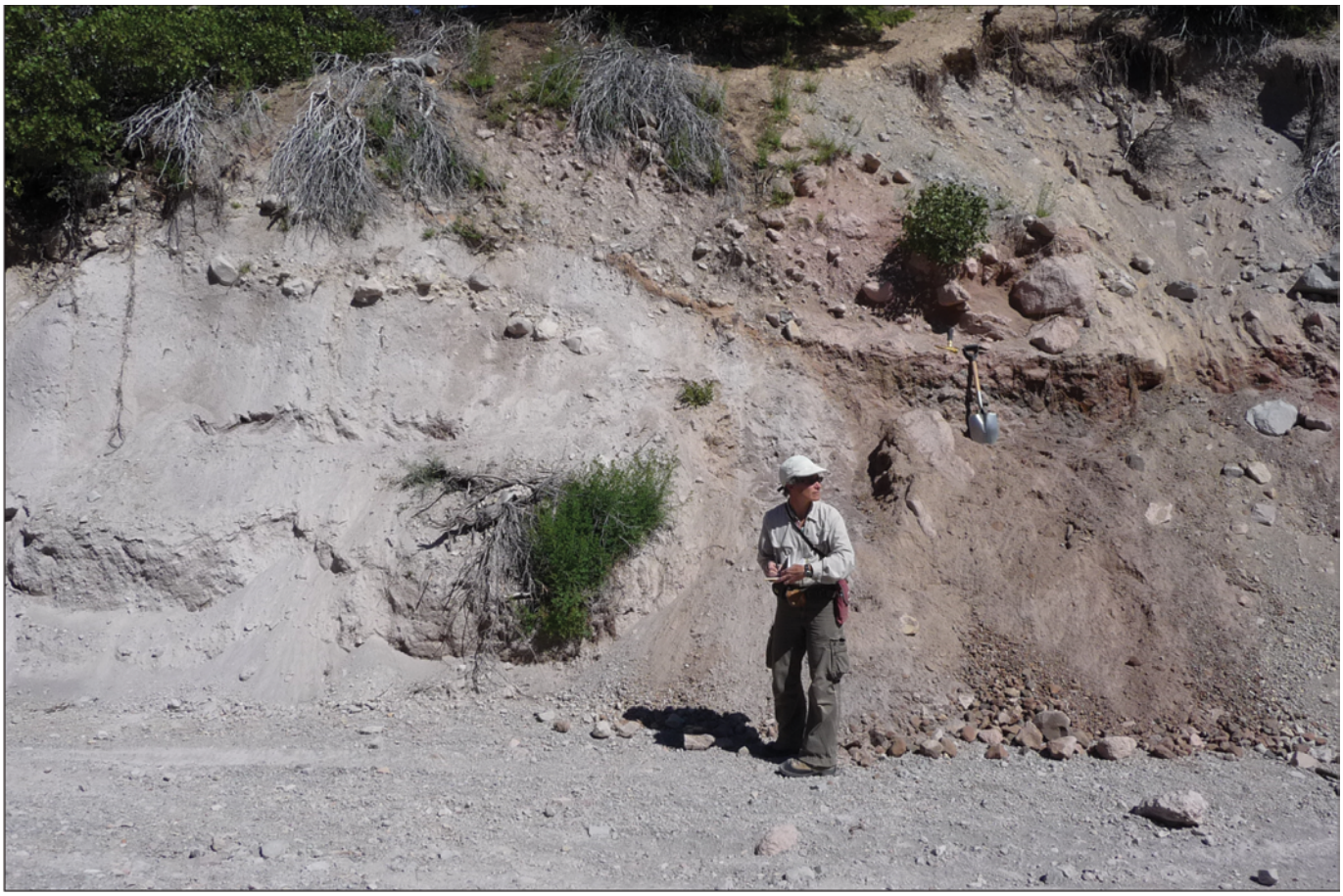

Figure 22. View of railroad cut at Stop 7, showing pyroclastic flows from Black Butte overlying others from the Shastina summit. Paleomagnetic measurements show that this entire section is slightly disturbed and rotated as a result of avalanching during emplacement of the Black Butte dome complex, yet it still perfectly preserves the stratigraphy of the two pyroclastic-flow units, which were deposited very closely in time.

Day 2—Regional Mafic Magmas North of Mount Shasta

0.0 From the street in front of the Tree House Motel in the City of Mount Shasta turn left onto Mount Shasta Boulevard and very shortly merge right onto Interstate 5 North. **8.6**

8.6 Take U.S. Hwy 97, Exit 747, then turn right into Weed. At the intersection with the second traffic light, merge right onto U.S. Hwy 97. Continue through Weed and beyond on U.S. Hwy 97, repeating the geology seen on this same road yesterday. **12.9**

21.5 On the left, pass Siskiyou County Road A12, the 97-99 cutoff to Grenada. **1.0**

22.5 Pass truck-parking spaces on both sides of U.S. Highway 97. In the middle distance ahead on the left (northeast) is Sheep Rock, a series of rough cliffs formed by Oligocene andesitic breccias that dip gently eastward. This is the southernmost exposure of Western Cascades volcanic rocks. At their base, though not visible from here, are Cretaceous marine sedimentary rocks that dip more steeply to the east. **1.3**

23.8 Roadcuts in the HAOT basalt of Pluto Cave (120 ka). **0.2**

24.0 Pass by the gravel Military Pass Road on the right (south), which leads to access points and a major trailhead for the north side of Mount Shasta. **0.7**

24.7 View on the right (east) of The Whaleback, a basaltic-andesite shield volcano of 103 ka, with a line of cinder cones along its summit ridge. Roadcuts just ahead expose an andesite flow that erupted from a flank vent on the north side of The Whaleback. **0.8**

25.5 Outcrops of the basalt of Pluto Cave. **0.5**

26.0 Turn right onto Deer Mountain Road (U.S. Forest Service Road 19). Pass through an underpass beneath the railroad tracks; continue eastward on this road, climbing to a saddle between two High Cascades shield volcanoes, The Whaleback on the right (south) and Deer Mountain on the left (north). The Whaleback and Deer Mountain are, respectively, younger (103 ka) and older (1.05 Ma) examples of short-lived calc-alkaline basaltic andesite and andesite shield volcanoes that erupted along the Cascade Arc axis. As is typical, these centers are homogeneous and appear short-lived, perhaps having erupted within a few thousands or tens of thousands of years, though their early parts are seldom exposed and have not been well studied. **3.9**

29.9 Where the paved road comes to a prominent saddle near a large paved parking lot on the right for a snowmobile park, turn left onto unpaved U.S. Forest Service Road 44N23. **0.5**

30.4 Drive the vehicles into a small offshoot track on the left and park.

Stop 8. HAOT basalt and high-Mg andesites exposed in The Whaleback-Deer Mountain saddle. (This stop has two parts, a pit crater here and a cinder cone near the snowmobile parking lot). Walk about 50 m from the vehicles to the rim of a pit crater, where there are outcrops of the high-alumina olivine tholeiite (HAOT) basalt of Pluto Cave and a view into the tree-filled crater. This is the southernmost of three aligned pit craters, just beyond which to the north (though not visible from here) is the rather inconspicuous eruptive vent for the basalt of Pluto Cave.

Turn vehicles around. Return to the paved road at the saddle, and park in the snowmobile parking lot just ahead. **0.5**

30.9 In addition to common arc andesites and basaltic andesites, such as The Whaleback and Deer Mountain, the large shield volcanoes both north and south of this saddle, two less common magma types erupted in the saddle: the basalt of Pluto Cave, a 120-ka HAOT basalt just seen at the pit crater, and high-Mg andesites that crop out intermittently on both sides of Deer Mountain road near the saddle. These andesites are similar to those shown by Grove and others (2003) to be one of several parental magma types for Mount Shasta lavas. The local eruptive source of the high-Mg andesites is a cinder cone on the south side of the saddle, the interior of which is well exposed in a quarry pit that is easily accessible on foot from this parking area. A trail that begins at the left (east) side of a warming hut at the end of the parking lot leads about 300 m into the cinder pit (fig. 23).

Exit the parking lot. From the saddle, continue on paved U.S. Forest Service Road 19, uphill around the east side of The Whaleback. Outcrops of basaltic andesite from the Whaleback are exposed intermittently along the road beyond here. **2.3**

33.2 Pass U.S. Forest Service Road 42N24 on the right, which can provide access to the upper part of The Whaleback. **0.9**

Figure 23. Stop 8, cinder-pit quarry in the Whaleback-Deer Mountain saddle. This cinder cone is the source of high-Mg andesite lava that flowed westward from the saddle, to and across U.S. Highway 97. The quarry exposes the internal structure of the cinder cone, including an apparent dike at the center, which is interpreted to be drainback of lava in the vent conduit at the end of the eruption. The composition of this high-Mg andesite probably is close to one of the parental magma types of the compositionally complex lavas of Mount Shasta.

34.1 A row of concrete barriers on the right (south) side of the road prevents loose debris from the roadcut above from spilling onto the road. Prominent outcrops in the lower part of the roadcut are basaltic andesite of The Whaleback. Above, the loose centimeter-sized fragments are 10.9-ka fallout pumice of Red Banks that erupted from near the present summit of Mount Shasta. **0.7**

34.8 Pull into the wide graded area along the left (southeast) side of the road, then walk downslope about 100 m along the same side of the road to a less obstructed view to the east. Exercise special caution while walking along this road, as it is frequented by logging trucks that cannot stop quickly for stray pedestrians.

Stop 9. Views into the Rainbow Mountain volcanic center (figs. 24 and 25). Deeply glaciated Butte Creek and Ash Creek Butte, to the east and south, and the Hotlum cone of Mount Shasta, to the southwest, are in view.

The Rainbow Mountain center (~900–1,300 ka) was a large stratovolcano located along the Cascade Arc axis. It forms the dissected high country immediately ahead and to the southeast. Its composition was similar to that of Mount Shasta. The edifice was at least as large as present-day Mount Shasta, based on the deep U-shaped valleys, likely dating from the glaciation of MIS 16 (~630 ka), that drained the now-eroded volcano.

Ash Creek Butte to the south is similar in size to The Whaleback. The eruption of Ash Creek Butte, however, was earlier (227 ka), and it has large glacial cirques on its north and east sides that contain moraines from glaciations of MIS 6 and MIS 2 (>130 and >17 ka, respectively).

(Although this trip does not do so, from here one can continue on this road about 6 miles farther to Military Pass on the east side of Mount Shasta for a closer view of the Hotlum cone. The paving ends a short way beyond here but a gravel road continues; shortly beyond the pavement end, take the right-hand fork across a ridge and down the far side into Military Pass. From there, a right turn onto the Military Pass dirt road leads northward around Mount Shasta and back to U.S. Hwy 97.)

Figure 24. Stop 9, view toward the southeast showing glaciated terrane of the Butte Creek drainage that deeply incises the Rainbow Mountain volcano, a stratocone of about 1 Ma that lies athwart the Cascades-Arc axis east of Mount Shasta. West Haight Mountain is a young cinder cone of augite basalt that erupted on the north rim of the valley of Alder Creek, a tributary of Butte Creek, and formed flows both to the east, out of view, and down over the north valley wall of Alder Creek onto its glaciated valley bottom.

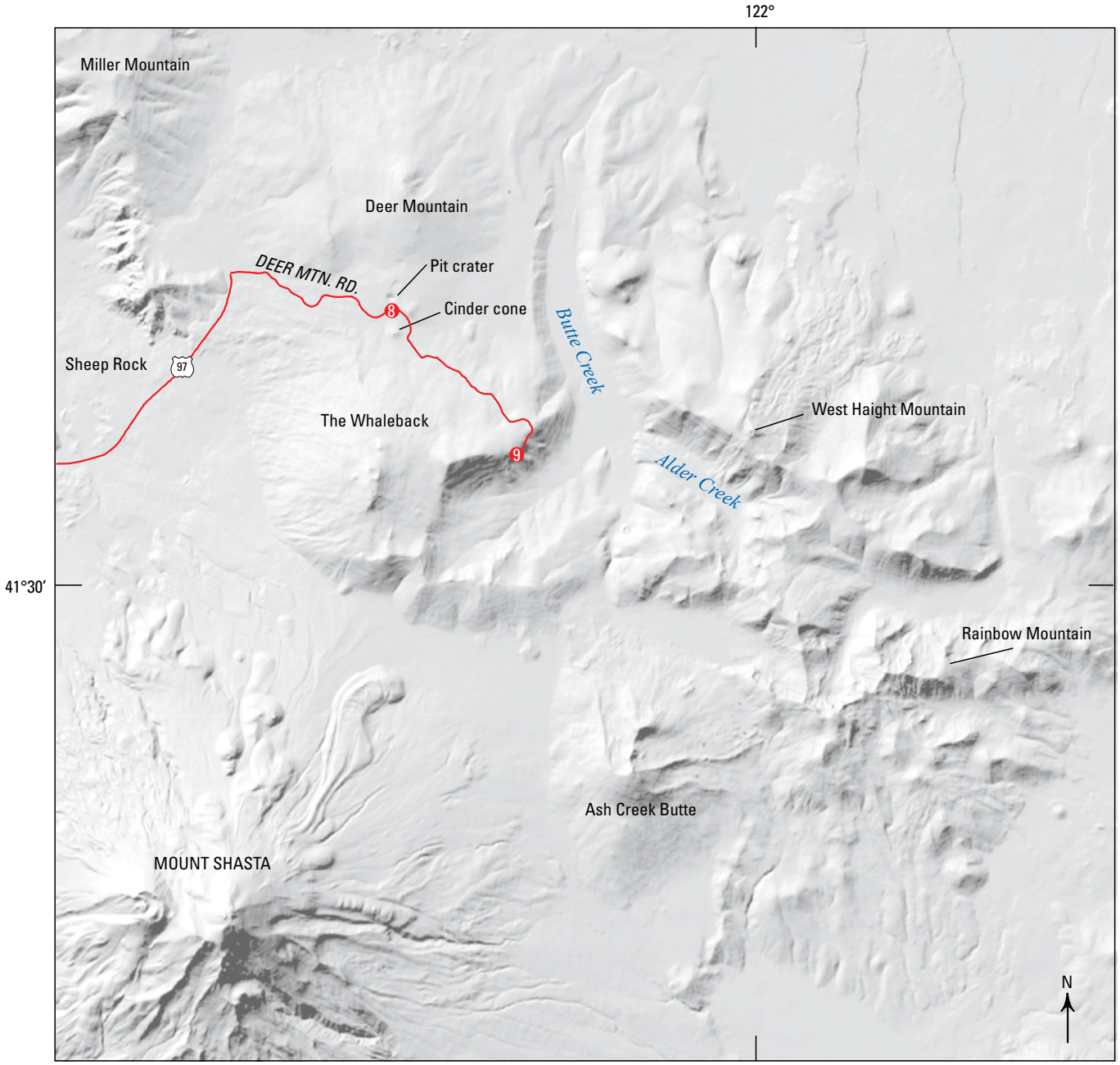

Figure 25. Digital-elevation model (DEM) of the area surrounding stops 8 and 9. The labeled pit crater at the first part of stop 8 can be seen to be in line with slightly less conspicuous craters just to its north-northeast. The cinder cone of stop 8 is the source for the lava flow on both sides of Deer Mountain Road. The view from stop 9 is across to Butte Creek, Alder Creek, Ash Creek Butte, and the distant Rainbow Mountain. Deep glacial valleys of MIS Stage 16 are seen to deeply incise the Rainbow Mountain stratovolcano, which forms most of the eroded terrain east and southeast of The Whaleback. See figure 1 for map area showing all stops.

Turn around and return by way of the roads just driven, back to U.S. Hwy 97. **3.8**

38.6 At the intersection with U.S. Hwy 97, turn left (south). The low hill directly ahead is the east side of Sheep Rock, on which andesite breccias of the Western Cascades here crop out only poorly. Farther toward the right is Miller Mountain, a Pliocene basaltic-andesite shield volcano with a prominent high point (Herd Peak) on which is located a U.S. Forest Service fire lookout. **0.4**

39.0 To the southwest is an excellent view of Mount Shasta. **0.8**

39.8 Roadcuts on both sides expose a north-flank andesite flow from The Whaleback. The view ahead (west) is toward Mount Eddy, an early Paleozoic ophiolitic complex in the eastern Klamath Mountains. **0.7**

40.5 Pass by the Military Pass Road on the left (south). **2.5**

43.0 Turn right (north) onto Siskiyou County Road A12 to Grenada. Views ahead of Miller Mountain and Sheep Rock. **1.6**

44.6 As the downhill gradient of the road decreases, we pass onto the surface of the HAOT basalt of Pluto Cave, exposed beyond here in intermittent outcrops, locally covered by runout from young debris flows of Mount Shasta. **2.5**

47.1 Pass Shasta View Road on the left (southwest). **0.9**

48.0 Pass Harry Cash Road on the right (north). **0.7**

48.7 Good roadcut exposure of the basalt of Pluto Cave. **1.3**

50.0 The low-relief valley floor here is covered by debris-flow runout from Mount Shasta. In the distance to the right (northwest), the sharp conical peak rising above the valley is an inlier of Western Cascades volcanic rocks. Farther around to the right, the crest of the High Cascades is formed by the volcanoes (right to left) Miller Mountain, Goosenest, and Willow Creek Mountain. **3.1**

53.1 Pass Juniper Lane on the left (south). The road ahead lies on basalt of Pluto Cave. Owlshead Mountain on the right (northwest) is a rhyolite of the Western Cascades. **1.1**

54.2 Pass the intersection with Siskiyou County Road A29 (Big Springs Road) on the left. Just beyond is the village of Big Springs. **2.7**

56.9 The road passes large blocks of the Shasta Valley avalanche deposit. Basalt of Pluto Cave continues to be exposed in low areas between the blocks. **3.2**

60.1 A bridge crosses the Shasta River, which here is reduced to merely an irrigation canal. Basalt of Pluto Cave continues to be exposed in low areas nearly to here, but this marks the west edge of the basalt. **1.0**

61.1 Cross a railroad track into the village of Grenada. **0.7**

61.8 Merge right onto Interstate 5. This marks the end of the Mount Shasta area field-trip guide.

References Cited

Bacon, C.R., Bruggman, P.E., Christiansen, R.L., Clynne, M.A., Donnelly-Nolan, J.M., and Hildreth, W., 1997, Primitive magmas at five Cascade volcanic fields—Melts from hot, heterogeneous sub-arc mantle: Canadian Mineralogist, v. 35, p. 397–423.

Baker, M.B., 1988, Evolution of lavas at Mt. Shasta volcano, northern California—An experimental and petrologic study: Massachussetts Institute of Technology, Ph.D. dissertation, 430 p.

Baker, M.B., Grove, T.L., and Price, R.C., 1994, Primitive basalts and andesites from the Mt. Shasta region, Northern California—Products of varying melt fraction and water content: Contributions to Mineralogy and Petrology, v. 118, p. 111–129.

Blakely, R.J., Christiansen, R.L., Ramsey, D.W., Smith, J.G., and Donnelly-Nolan, J.M., 2000, A three-dimensional view of Mt. Shasta, California, based on inversion of gravity anomalies: Geological Society of America Abstracts with Programs, v. 32, no. 7, p. A–430.

Clark, D., Gillespie, A.R., Clark, M., and Burke, B., 2003, Mountain glaciations of the Sierra Nevada, *in* Easterbrook, D.J., ed., Quaternary geology of the United States, INQUA 2003 field guide volume: Reno, Nev., Desert Research Institute, p. 287–311.

Crandell, D.R., 1989, Gigantic debris avalanche of Pleistocene age from ancestral Mount Shasta volcano, California, and debris-avalanche hazard zonation: U.S. Geological Survey Bulletin 1861, p. 32.

Dean, W.E., Kennett, J.P., Behl, R.J., and Nicholson, 2015, Abrupt termination of Marine Isotope Stage 16 (Termination VII) at 631.5 ka in Santa Barbara Basin, California: Paleoceanography, v. 30, no. 10, p. 1373–1390.

Finch, R.H., 1930, Activity of a California volcano in 1786: The Volcano Letter, no. 308, p. 3.

Fuis, G.S., Zucca, J.J., Mooney, W.D., and Milkereit, B., 1987, A geologic interpretation of seismic-refraction results in northeastern California: Geological Society of America Bulletin, v. 98, no. 1, p. 53–65.

Gardner, C.A., Champion, D.E., Christiansen, R.L., Calvert, A.T., and Mosbrucker, A.R., 2013, Paleomagnetic constraints on the timing and duration of latest Pleistocene to early Holocene eruptions at Mount Shasta volcano, California, USA: American Geophysical Union abstracts for 2013 Fall Meeting, abstract V13G-2706.

Grove, T.L., Elkins-Tanton, L.T., Parman, S.W., Chatterjee, N., Müntener, O., and Gaetani, G.A., 2003, Fractional crystallization and mantle-melting controls on calc-alkaline differentiation trends: Contributions to Mineralogy and Petrology, v. 145, p. 515–533.

Grove, T.L., Parman, S.W., Bowring, S.A., Price, R.C., and Baker, M.B., 2002, The role of an H_2O-rich fluid component in the generation of primitive basaltic andesites and andesites from the Mt. Shasta region, northern California: Contributions to Mineralogy and Petrology, v. 142, p. 375–396.

Grove, T. L., Baker, M.B., Price, R.C., Parman, S.W., Elkins-Tanton, L.T., Chatterjee, N., and Müntener, O., 2005, Magnesian andesite and dacite lavas from Mount Shasta, northern California—products of fractional crystallization of H_2O-rich mantle melts: Contributions to Mineralogy and Petrology, v. 148, p. 542–565.

Guffanti, Marianne, and Weaver, C.S., 1988, Distribution of late Cenozoic volcanic vents in the Cascade Range (USA)—Volcanic-arc segmentation and regional tectonic considerations: Journal of Geophysical Research, v. 93, p. 6515 and fig. 6.

Harris, S.L., 1988, Fire mountains of the west—The Cascade and Mono Lake volcanoes: Missoula, Mont., Mountain Press, 379 p.

Hildreth, Wes, 2007, Quaternary magmatism in the Cascades—Geologic perspectives: U.S. Geological Survey Professional Paper 1744, p. 34.

Hill, M., and Egenhoff, E.L., 1976, A California jökulhlaup: California Geology, v. 29, no. 7, p. 154–158.

Krawczynski, M.J., Grove, T.L., Medard, E., Barr, J.A., Till, C.B., and Behrens, H., 2006, The fate of wet mantle melts—Fractional crystallization processes preserved in magmatic inclusions, Mt. Shasta, CA: Eos Transactions of the American Geophysical Union, v. 87, Fall Meeting Supplement, Abstract V14B-06.

LaFehr, T.R., 1965, Gravity, isostasy, and crustal structure in the southern Cascade Range: Journal of Geophysical Research, v. 70, p. 5581–5597.

Lisiecki, L.E., and Raymo, M.E., 2005, A Pliocene–Pleistocene stack of 57 globally distributed benthic $\delta^{18}O$ records: Paleoceanography, v. 20, p. PA1003.

Masson, P.H., 1949, Circular soil structures in northeastern California: California Division of Mines Bulletin 151, p. 61–71.

McCanta, M.C., Rutherford, M.J., and Hammer, J.E., 2007, Pre-eruptive and syn-eruptive conditions in the Black Butte, California, dacite—Insight into crystallization kinetics in a silicic magma system: Journal of Volcanology and Geothermal Research, v. 16, p. 263–284.

McCrory, P.A., Blair, J.L., Waldhauser, F., and Oppenheimer, D.H., 2012, Juan de Fuca slab geometry and its relation to Wadati-Benioff zone seismicity: Journal of Geophysical Research, v. 117, no. B09306, p. 23.

Pakiser, L.C., 1964, Gravity, volcanism, and crustal structure in the southern Cascade Range, California: Geological Society of America Bulletin, v. 75, p. 611–620.

Ui, T., and Glicken, H., 1986, Internal structural variations in a debris-avalanche deposit from ancestral Mount Shasta, California, USA: Bulletin of Volcanology, v. 48, p. 189–194.

Zucca, J.J., Fuis, G.S., Milkereit, B., Mooney, W.D., and Catchings, R., 1986, Crustal structure of northern California from seismic refraction data: Journal of Geophysical Research, v. 91, p. 7359–7382.

Menlo Park Publishing Service Center, California
Manuscript approved June 2, 2017
Edited by Jan Zigler
Layout by Cory Hurd

ISSN 2328-0328 (online)
https://doi.org/10.3133/sir20175022K3